

“ANALYSIS AND DESIGN OF A SOLAR CHARGE CONTROLLER USING CUK CONVERTER”

Major Project Report

*Submitted in Partial Fulfillment of the Requirements
for the degree of*

MASTER OF TECHNOLOGY

IN

ELECTRICAL ENGINEERING

(Power Electronics, Machines and Drives)

By

Mrunal Makwana

12MEEP43



**DEPARTMENT OF ELECTRICAL ENGINEERING
INSTITUTE OF TECHNOLOGY
NIRMA UNIVERSITY
AHMEDABAD-382481**

May 2014

Certificate

This is to certify that the Major Project Report entitled “Analysis and Design of a Solar Charge Controller Using Cuk Converter” submitted by **Mr. Mrunal Makwana (Roll No: 12MEEP43)** towards the partial fulfillment of the requirements for Master of Technology (Electrical Engineering) in the field of Power Electronics, Machines & Drives of Nirma University is the record of work carried out by him under our supervision and guidance. The work submitted has in our opinion reached a level required for being accepted for examination. The results embodied in this major project work to the best of our knowledge have not been submitted to any other University or Institution for award of any degree or diploma.

Date:

Industrial Guide

Mr. M. R. Tilwalli

Proprietor

Gururaj Engineers

G.I.D.C. Makarpura

Vadodara

Institute Guide

Professor M. C. Shah

Department of Electrical Engg.

Institute of Technology

Nirma University

Ahmedabad

Head of Department

Department of Electrical Engg.

Institute of Technology

Nirma University

Ahmedabad

Director

Institute of Technology

Nirma University

Ahmedabad

Undertaking for Originality of the Work

I **Mrunal Makwana**, Roll No. **12MEEP43**, give undertaking that the Major Project entitled “**Analysis and Design of a Solar Charge Controller Using Cuk Converter**” submitted by me, towards the partial fulfillment of the requirements for the degree of Master of Technology in **Power Electronics Machines & Drives, Electrical Engineering**, under Institute of Technology of Nirma University, Ahmedabad, is the original work carried out by me and I give assurance that no attempt of plagiarism has been made. I understand that in the event of any similarity found subsequently with any published work or any dissertation work elsewhere; it will result in severe disciplinary action.

.....

Signature of Student

Date:

Place:

Endorsed by:

.....

(Signature of Project Guide)

Prof. Mihir Shah

Assistant Professor

Department of Electrical Engineering

Institute of Technology

Nirma University

Ahmedabad

Acknowledgement

I would like to express my sincere thanks to my Industry guide Mr M.R. Tilwalli, Proprietor, Gururaj Engineers, G.I.D.C, Makarpura, Vadodara, for his constant support, timely help, guidance, sincere co-operation during the entire period of my work. I am grateful to him for providing all the necessary facilities during the course of the project work.

I would also like to thank my Institute guide Prof. Mihir Shah, Department of Electrical Engineering, Institute of Technology, Nirma University, Ahmedabad for the help provided during various stages of the project.

I am thankful to Dr. P.N.Tekwani (HOD, EE Dept.) for allowing me to do my project work at Gururaj Engineers, G.I.D.C, Makarpura, Vadodara.

I would like to thank my colleague and friend Utkarsh Panchal for his support and willingness to help me out during various stages of my project. Also, thanks to,, Meet Patel, Ashwini Kumar, Ritesh Gosai and all other Institute colleagues for their kind support. Furthermore I am grateful to all the employees of Gururaj Engineers for their constant efforts.

Finally, to my parents, my brother, and my friends - many thanks for much support the whole way through, for constant encouragement and support during two years of my graduate work.

Mrunal Makwana

May 2014

Abstract

Dynamic analysis and design of Cuk converter in parallel power transfer (PPT) configuration for solar charger controller application is presented. In this configuration Cuk converter has step down regulation therefore it is suitable for system with low battery voltage rating with high voltage PV modules. In order to extract maximum power from PV modules a modified power-current (P-I) based MPPT is used along with PWM control. In such MPPT circuit low current ripple in input is needed to track maximum power accurately. This can be satisfied by Cuk converter which has both continuous current in input and output. The simulation results are presented and analyzed to validate that the proposed simulation model is effective for MPPT control of the photovoltaic systems at rapidly changing irradiation condition. Experiment is conducted to verify the overall system performance in extracting power from PV modules.

Abbreviations

MPPT	Maximum Power Point Tracking
PWM	Pulse Width Modulation
PV	Photovoltaic
ESR	Equivalent Series Resistance
KVL	Kirchoff's Voltage Law
IEEE	Institute of Electrical and Electronic Engineers
PPT	Parallel Power Transfer
P&O	Perturb and Observe
PIC	Programmable Interface Controller
PLL	Phase Locked Loop
ADC	Analog to Digital Converter
SMPS	Switch Mode Power Supply
DSP	Digital Signal Processor

Nomenclature

I	Solar cell's output current
V	Solar cell's output voltage
T	Solar cell's temperature
I_{OS}	Solar cell's reverse saturation current
k	Boltzmann's constant
q	electronic charge
A	sunlight intensity
I_{SCR}	Short circuit current
I_{LG}	current produce by light
K_i	temperature coefficient under short circuit current
E_{go}	silicon bandwith
T_r	reference temperature
I_{or}	Solar cell's saturation current
R_{sh}	equivalent parallel resistance
R_s	equivalent series resistance
D	duty cycle
f	switching frequency
T	switching period
V_s	input voltage
V_o	output voltage
P_s	input power
P_o	output power
I_s	input current
I_o	output current
V_{MPP}	voltage at maximum power point
I_{MPP}	current at maximum power point

Contents

Certificate	ii
Undertaking	iii
Acknowledgement	iv
Abstract	v
Abbreviations/Nomenclature	vi
List of Figures	x
List of Tables	xi
1 Introduction	2
1.1 Problem Identification	2
1.2 Definition	3
1.3 Objective	4
2 Solar Cell Modelling	5
2.1 Basic Model	5
2.2 Effect Of Variation Of Solar Irradiation	6
2.3 Effect Of Variation Of Temperature	7
3 Maximum Power Point Tracking	10
3.1 Introduction	10
3.2 Methods Of MPPT	10
3.2.1 Perturb and Observe method	11
3.2.2 Incremental Conductance method	11
3.2.3 Parasitic Capacitance method	12
3.2.4 Constant Voltage method	12
3.2.5 Constant Current method	12
3.2.6 Flowchart of Incremental Conductance Algorithm	13

4 Cuk Converter	15
4.1 Waveforms	16
4.2 Operation of Cuk Converter	16
4.3 Mechanism of Load Matching	20
5 The Proposed System	23
6 Design and Simulations	25
6.1 Introduction	25
6.2 Cuk Converter Design	25
6.2.1 Calculations	26
6.3 Simulation and Results	28
7 Hardware Description	38
7.1 Cuk Converter	38
7.1.1 MOSFET IRF540N	39
7.1.2 Schottky Diode	39
7.2 Control Circuit Configuration	41
8 Experimental Results	43
9 Conclusion	47
9.1 Summary	47
9.2 Future Scope	47
References	48
Appendix	50

List of Figures

2.1	Single diode model of a Solar Cell	6
2.2	P-V I-V curve of a solar cell at given temperature and solar irradiation	7
2.3	Variation of P-V curve with solar irradiation	8
2.4	Variation of I-V curve with solar irradiation	8
2.5	Variation of P-V curve with temperature	9
2.6	Variation of I-V with temperature	9
3.1	Flowchart of the Incremental Conductance Algorithm	14
3.2	Basic concept of Incremental Conductance on a PV curve	14
4.1	Circuit of Cuk Converter	15
4.2	Waveforms of Cuk Converter	17
4.3	Cuk Converter when the switch is ON	18
4.4	Cuk Converter when the switch is OFF	19
4.5	The impedance seen by PV is R_{in} that is adjustable by duty cycle (D)	21
5.1	Power flow of converter in (a) conventional and (b) PPT configuration.	24
5.2	Cuk converter in PPT configuration for solar charge controller application.	24
6.1	Simulation model of the PV module	29
6.2	Subsystem of the PV module	29
6.3	Simulink model of entire system with MPPT	30
6.4	Subsystem of the cuk converter	30
6.5	Subsystem of Incremental Conductance MPPT algorithm	31
6.6	PV & IV curve of solar model	31
6.7	IV curves under different solar Irradiations(W/m^2) at $25^\circ C$	32
6.8	PV curves under different solar Irradiations(W/m^2) at $25^\circ C$	32
6.9	Gating signal from MPPT module	33
6.10	Voltage(V_{C1}, V_{C2}) & Current(I_{L1}, I_{L2}) of the Cuk Converter	33
6.11	Output voltage of the Cuk Converter	34
6.12	Output current of the Cuk Converter	34
6.13	Comparison of the both powers P_{in} and P_{out} (without closed loop) . .	35
6.14	Comparison of the both powers P_{in} and P_{out} (with closed loop) . . .	35

6.15	PIC simulation diagram	36
6.16	Pulses obtained from PIC controller	37
7.1	Pin configuration of IRF540N	40
7.2	Driver circuit for MOSFET	40
7.3	Pin diagram of LA25-NP	41
7.4	Pin configuration of PIC16F887	41
8.1	Pulses obtained from PIC controller [Scale:X-axis 1cm=25 μ s/div Y-axis 1cm=5V/div]	44
8.2	Solar Panel current sensed from LEM current sensor	44
8.3	Solar Panel voltage	45
8.4	Pulses from the driver circuit [Scale:X-axis 1cm=50 μ s/div Y-axis 1cm=5V/div]	45
8.5	Output Voltage of the Cuk Converter	46

List of Tables

I	Load matching with resistive load (6Ω) under the varying irradiance .	22
II	Load matching with resistive load (12Ω) under the varying irradiance	22

Chapter 1

Introduction

One of the major concerns in the power sector is the day-to-day increasing power demand but the unavailability of enough resources to meet the power demand using the conventional energy sources. Demand has increased for renewable sources of energy to be utilized along with conventional systems to meet the energy demand. Renewable sources like wind energy and solar energy are the prime energy sources which are being utilized in this regard. The continuous use of fossil fuels has caused the fossil fuel deposit to be reduced and has drastically affected the environment depleting the biosphere and cumulatively adding to global warming[1].

1.1 Problem Identification

Solar energy is abundantly available that has made it possible to harvest it and utilize it properly. Solar energy can be a stand alone generating unit or can be a grid connected generating unit depending on the availability of a grid nearby. Thus it can be used to power rural areas where the availability of grids is very low. Another advantage of using solar energy is the portable operation whenever wherever necessary.

In order to tackle the present energy crisis one has to develop an efficient manner in which power has to be extracted from the incoming solar radiation. The power

conversion mechanisms have been greatly reduced in size in the past few years. The development in power electronics and material science has helped engineers to come up with very small but powerful systems to withstand the high power demand. But the disadvantage of these systems is the increased power density. Trend has set in for the use of multi-input converter units that can effectively handle the voltage fluctuations. But due to high production cost and the low efficiency of these systems they can hardly compete in the competitive markets as a prime power generation source.

The constant increase in the development of the solar cells manufacturing technology would definitely make the use of these technologies possible on a wider basis than what the scenario is presently. The use of the newest power control mechanisms called the Maximum Power Point Tracking (MPPT) algorithms has led to the increase in the efficiency of operation of the solar modules and thus is effective in the field of utilization of renewable sources of energy.

1.2 Definition

A charge controller, or charge regulator is basically a voltage and/or current regulator to keep batteries from overcharging. It regulates the voltage and current coming from the solar panels going to the battery. Most 12 V panels put out about 16 to 20 V, so if there is no regulation the batteries will be damaged from overcharging. Most batteries need around 14 to 14.5 V to get fully charged. Charge controllers are sold to consumers as separate devices, often in conjunction with solar or wind power generators, for uses such as RV, boat, and off-the-grid home battery storage systems. In solar applications, charge controllers may also be called solar regulators. Some charge controllers / solar regulators have additional features, such as a low voltage disconnect, a separate circuit which powers down the load when the batteries become overly discharged (some battery chemistries are such that over-discharge can ruin the battery). A series charge controller or series regulator disables further current flow into batteries when they are full. A shunt charge controller or shunt regulator diverts

excess electricity to an auxiliary or shunt load, such as an electric water heater, when batteries are full. Simple charge controllers stop charging a battery when they exceed a set high voltage level, and re-enable charging when battery voltage drops back below that level. Pulse width modulation (PWM) and maximum power point tracker (MPPT) technologies are more electronically sophisticated, adjusting charging rates depending on the battery's level, to allow charging closer to its maximum capacity. Charge controllers may also monitor battery temperature to prevent overheating. Some charge controller systems also display data, transmit data to remote displays, and data logging to track electric flow over time.

1.3 Objective

The basic objective would be to study MPPT and successfully implement the MPPT algorithms using the simulation models. Modeling the converter and the solar cell in simulation and interfacing both with the MPPT algorithm to obtain the maximum power point operation would be of prime importance.

Chapter 2

Solar Cell Modelling

This chapter discusses the fundamentals of PV cells and modeling of a PV cell using an equivalent electrical circuit. The models are implemented to study PV characteristics and simulate a real PV module.

2.1 Basic Model

A solar cell is the building block of a solar panel. A photovoltaic module is formed by connecting many solar cells in series and parallel. Considering only a single solar cell; it can be modeled by utilizing a current source, a diode and two resistors. This model is known as a single diode model of solar cell. Two diode models are also available but only single diode model is considered here.[3]

The characteristic equation for a photovoltaic cell is given by

$$I_{LG} - I_{OS} \left[\exp\left(\frac{q}{AkT}(V + IR_s)\right) - 1 \right] - \frac{V + IR_s}{R_{sh}} \quad (2.1)$$

where

$$I_{os} = I_{or} \left(\frac{T}{T_r}\right)^3 \left[\exp\left(\frac{qE_{go}}{Ak}\right) \left(\frac{1}{T_r} - \frac{1}{T}\right) \right] \quad (2.2)$$

$$I_{LG} = [I_{SCR} + K_i(T - 25)] \frac{\lambda}{100} \quad (2.3)$$

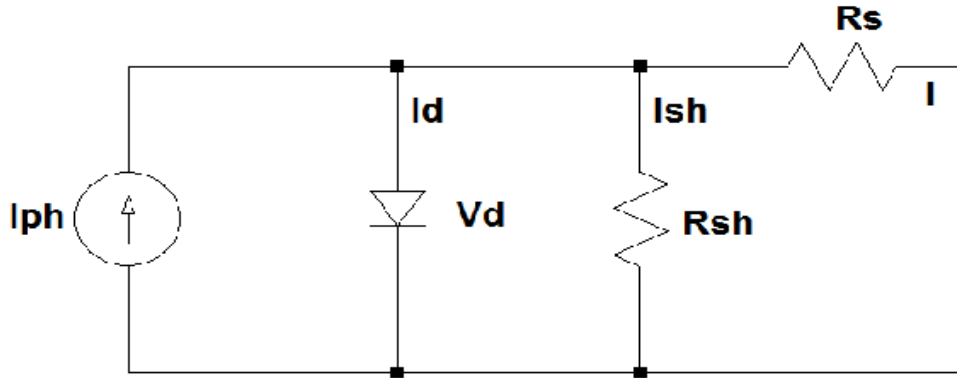


Figure 2.1: Single diode model of a Solar Cell

Where I and V is solar cell's output current and voltage respectively, I_{OS} is solar cell's reverse saturation current, T is solar cell's temperature($^{\circ}\text{C}$), k is the Boltzmann constant, q is electronic charge, A is sunlight intensity(W/m), I_{SCR} is short-circuit current at 25°C and $1000(\text{W}/\text{m})$, I_{LG} is current produced by light, $K_i = 0.0017 \text{ A}/^{\circ}\text{C}$, which is temperature coefficient under short-circuit current I_{SCR} , E_{go} is silicon bandwidth, $B=A=1.92$, which is a ideal coefficient, $T_r=301.18 \text{ }^{\circ}\text{C}$, which is the reference temperature, I_{or} is solar cell's saturation current at T_r , R_{sh} is equivalent parallel resistance, R_s is equivalent series resistance(ESR).

The I-V and P-V curves for a solar cell are given in the following figure. It can be seen that the cell operates as a constant current source at low values of operating voltages and a constant voltage source at low values of operating current.

2.2 Effect Of Variation Of Solar Irradiation

The P-V and I-V curves of a solar cell are highly dependent on the solar irradiation values. The solar irradiation as a result of the environmental changes keeps on fluctuating, but control mechanisms are available that can track this change and can alter

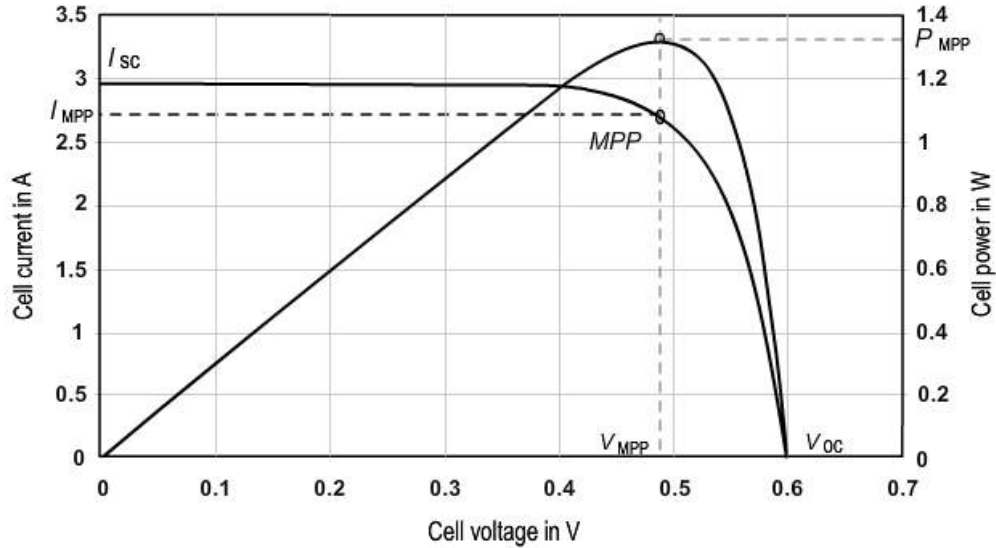


Figure 2.2: P-V I-V curve of a solar cell at given temperature and solar irradiation

the working of the solar cell to meet the required load demands. Higher is the solar irradiation, higher would be the solar input to the solar cell and hence power magnitude would increase for the same voltage value. With increase in the solar irradiation the open circuit voltage increases. This is due to the fact that, when more sunlight incidents on to the solar cell, the electrons are supplied with higher excitation energy, thereby increasing the electron mobility and thus more power is generated.

2.3 Effect Of Variation Of Temperature

On the contrary the temperature increase around the solar cell has a negative impact on the power generation capability. Increase in temperature is accompanied by a decrease in the open circuit voltage value. Increase in temperature causes increase in the band gap of the material and thus more energy is required to cross this barrier. Thus the efficiency of the solar cell is reduced.

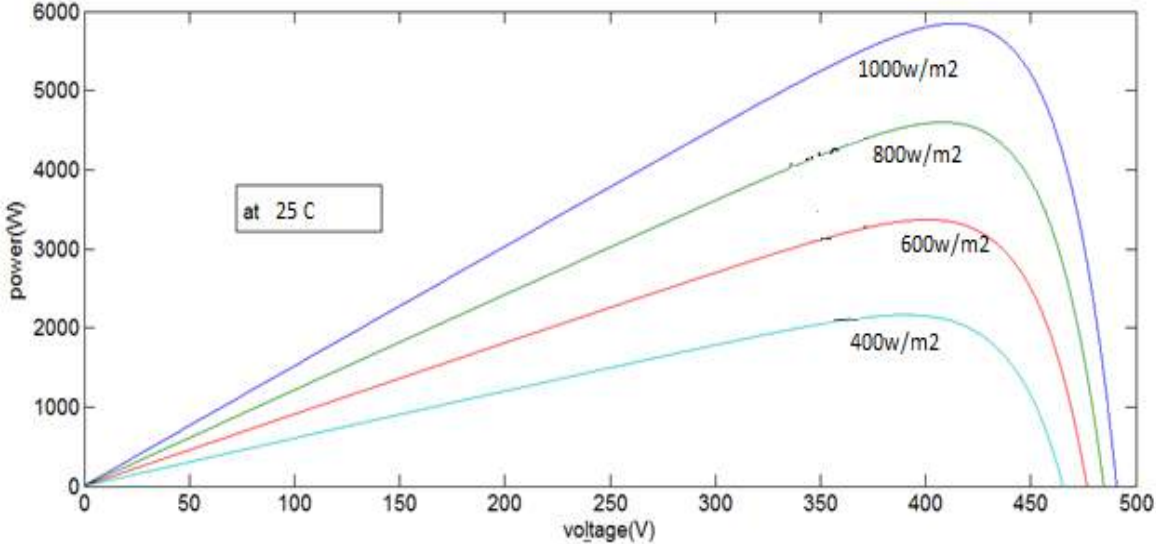


Figure 2.3: Variation of P-V curve with solar irradiation

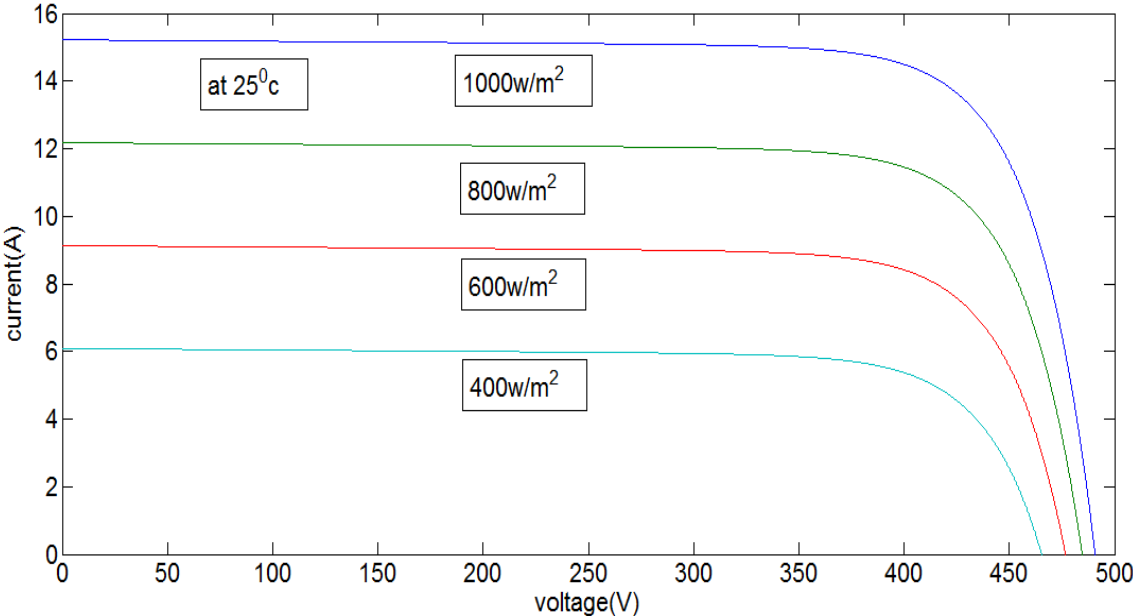


Figure 2.4: Variation of I-V curve with solar irradiation

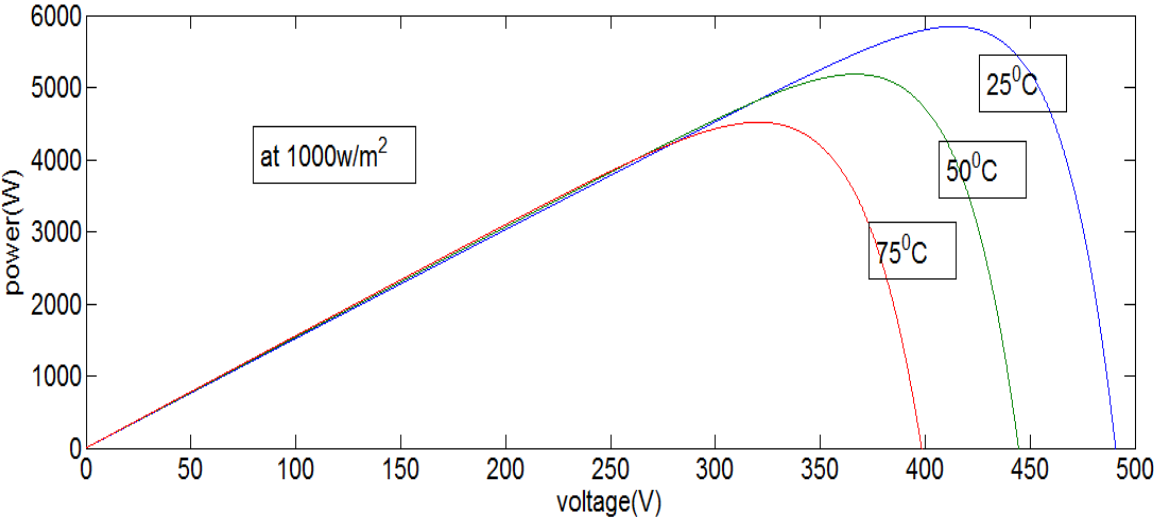


Figure 2.5: Variation of P-V curve with temperature

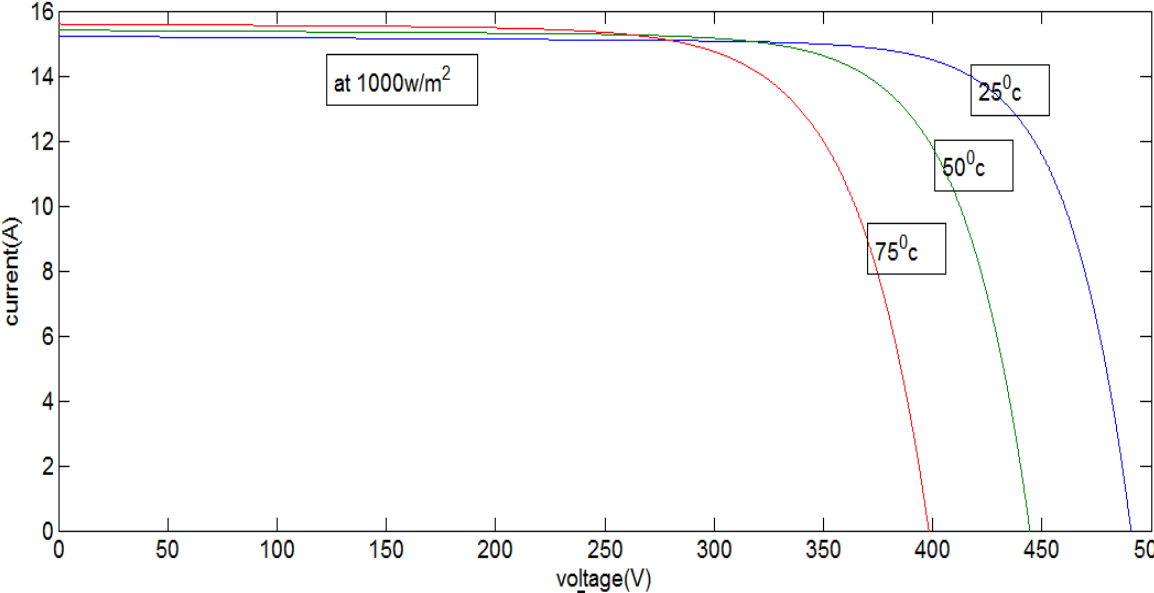


Figure 2.6: Variation of I-V with temperature

Chapter 3

Maximum Power Point Tracking

3.1 Introduction

The maximum power point tracker (MPPT) is now prevalent in grid-tied PV power systems and is becoming more popular in stand-alone systems. It should not be confused with sun trackers, mechanical devices that rotate and/or tilt PV modules in the direction of sun. MPPT is a power electronic device interconnecting a PV power source and a load, maximizes the power output from a PV module or array with varying operating conditions, and therefore maximizes the system efficiency. MPPT is made up with a switch-mode DC-DC converter and a controller. For grid-tied systems, a switch-mode inverter sometimes fills the role of MPPT. Otherwise, it is combined with a DC-DC converter that performs the MPPT function.[4]

3.2 Methods Of MPPT

There are many methods used for maximum power point tracking, a few are listed below:[5]

- Perturb and Observe method
- Incremental Conductance method

- Parasitic Capacitance method
- Constant Voltage method
- Constant Current method

3.2.1 Perturb and Observe method

This method is the most common. In this method very less number of sensors are utilized . The operating voltage is sampled and the algorithm changes the operating voltage in the required direction and samples $\frac{dP}{dV}$. If $\frac{dP}{dV}$ is positive, then the algorithm increases the voltage value towards the MPP until $\frac{dP}{dV}$ is negative. This iteration is continued until the algorithm finally reaches the MPP. This algorithm is not suitable when the variation in the solar irradiation is high. The voltage never actually reaches an exact value but perturbs around the maximum power point (MPP).

3.2.2 Incremental Conductance method

This method uses the PV array's incremental conductance $\frac{dI}{dV}$ to compute the sign of $\frac{dP}{dV}$. When $\frac{dI}{dV}$ is equal and opposite to the value of I/V (where $\frac{dP}{dV}=0$) the algorithm knows that the maximum power point is reached and thus it terminates and returns the corresponding value of operating voltage for MPP. This method tracks rapidly changing irradiation conditions more accurately than P and O method. One complexity in this method is that it requires many sensors to operate and hence is economically less effective.

$$P = V * I \quad (3.1)$$

Differentiating with respect to voltage yields;

$$\frac{dP}{dV} = \frac{d(V * I)}{dV} \quad (3.2)$$

$$\frac{dP}{dV} = I * \left(\frac{dV}{dV}\right) + V * \left(\frac{dI}{dV}\right) \quad (3.3)$$

$$\frac{dP}{dV} = I + V * \left(\frac{dI}{dV}\right) \quad (3.4)$$

When the maximum power point is reached the slope $\frac{dP}{dV}=0$, the condition would be

$$\frac{dP}{dV} = 0 \quad (3.5)$$

$$I + V * \left(\frac{dI}{dV}\right) = 0 \quad (3.6)$$

$$\frac{dI}{dV} = -\frac{I}{V} \quad (3.7)$$

3.2.3 Parasitic Capacitance method

This method is an improved version of the incremental conductance method, with the improvement being that the effect of the PV cell's parasitic union capacitance is included into the voltage calculation.

3.2.4 Constant Voltage method

This method which is a not so widely used method because of the losses during operation is dependent on the relation between the open circuit voltage and the maximum power point voltage. The ratio of these two voltages is generally constant for a solar cell, roughly around 0.76. Thus the open circuit voltage is obtained experimentally and the operating voltage is adjusted to 76% of this value.

3.2.5 Constant Current method

Similar to the constant voltage method, this method is dependent on the relation between the open circuit current and the maximum power point current. The ratio of these two currents is generally constant for a solar cell, roughly around 0.95. Thus the short circuit current is obtained experimentally and the operating current is adjusted to 95% of this value.

The methods have certain advantages and certain disadvantages. Choice is to be made regarding which algorithm to be utilized looking at the need of the algorithm and the operating conditions. For example, if the required algorithm is to be simple and not much effort is given on the reduction of the voltage ripple then P and O is suitable. But if the algorithm is to give a definite operating point and the voltage fluctuation near the MPP is to be reduced then the IC method is suitable, but this would make the operation complex and more costly.

3.2.6 Flowchart of Incremental Conductance Algorithm

In 1993 Hussein, Muta, Hoshino, and Osakada of Saga University, Japan, proposed the incremental conductance algorithm intending to solve the problem of the P&O algorithm under rapidly changing atmospheric conditions. The basic idea is that the slope of P-V curve becomes zero at the MPP, as shown in Figure 3.1. It is also possible to find a relative location of the operating point to the MPP by looking at the slopes. The slope is the derivative of the PV modules power with respect to its voltage.

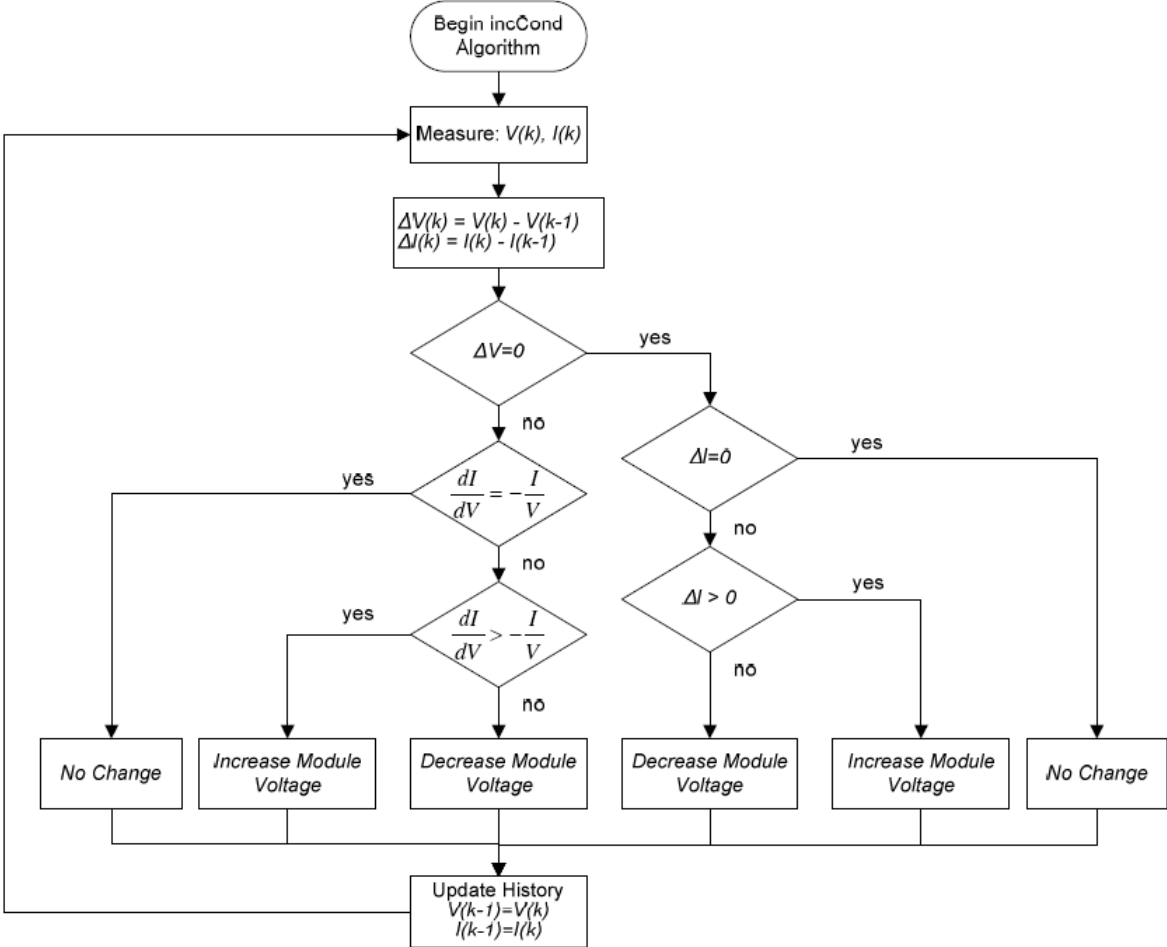


Figure 3.1: Flowchart of the Incremental Conductance Algorithm

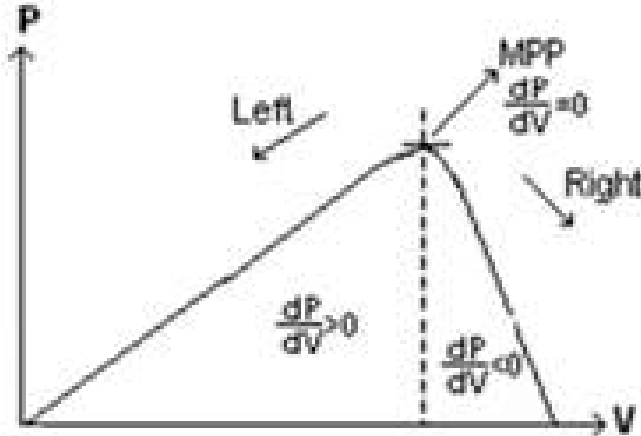


Figure 3.2: Basic concept of Incremental Conductance on a PV curve

Chapter 4

Cuk Converter

The circuit of the Cuk converter is shown in Fig. 4.1. It consists of dc input voltage source V_S , input inductor L_1 , controllable switch S , energy transfer capacitor C_1 , diode D , filter inductor L_2 , filter capacitor C_2 , and load resistance R . [2] An important

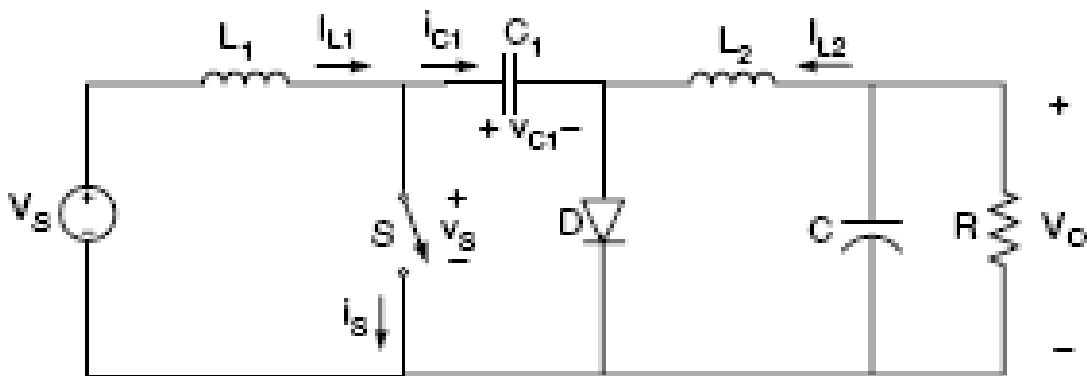


Figure 4.1: Circuit of Cuk Converter

advantage of this topology is a continuous current at both the input and the output of the converter. Disadvantages of the Cuk converter include a high number of reactive components and high current stresses on the switch, the diode, and the capacitor C_1 . Main waveforms in the converter are presented in Fig.4.2.

4.1 Waveforms

When the switch is on, the diode is off and the capacitor C_1 is discharged by the inductor L_2 current. With the switch in the off state, the diode conducts currents of the inductors L_1 and L_2 whereas capacitor C_1 is charged by the inductor L_1 current. To obtain the dc voltage transfer function of the converter, we shall use the principle that the average current through a capacitor is zero for steady-state operation. Let us assume that inductors L_1 and L_2 are large enough that their ripple current can be neglected. Capacitor C_1 is in steady state if,

$$I_{L2}DT = I_{L1}(1 - D)T \quad (4.1)$$

For a lossless converter

$$P_s = V_s I_{L1} = -V_o I_{L2} = P_o \quad (4.2)$$

Combining these two equations, the dc voltage transfer function of the Cuk converter is

$$M_v = \frac{V_o}{V_s} = \frac{-D}{1 - D} \quad (4.3)$$

4.2 Operation of Cuk Converter

The basic operation of Ck converter in continuous conduction mode is explained here. In steady state, the average inductor voltages are zero, thus by applying Kirchoffs voltage law (KVL) around outermost loop of the circuit shown in Figure 4.1.[6]

$$V_{C1} = V_s + V_o \quad (4.4)$$

Assume the capacitor (C_1) is large enough and its voltage is ripple free even though it stores and transfer large amount of energy from input to output. The initial condition is when the input voltage is turned on and switch (SW) is off. The diode (D) is forward biased, and the capacitor (C_1) is being charged. The operation of

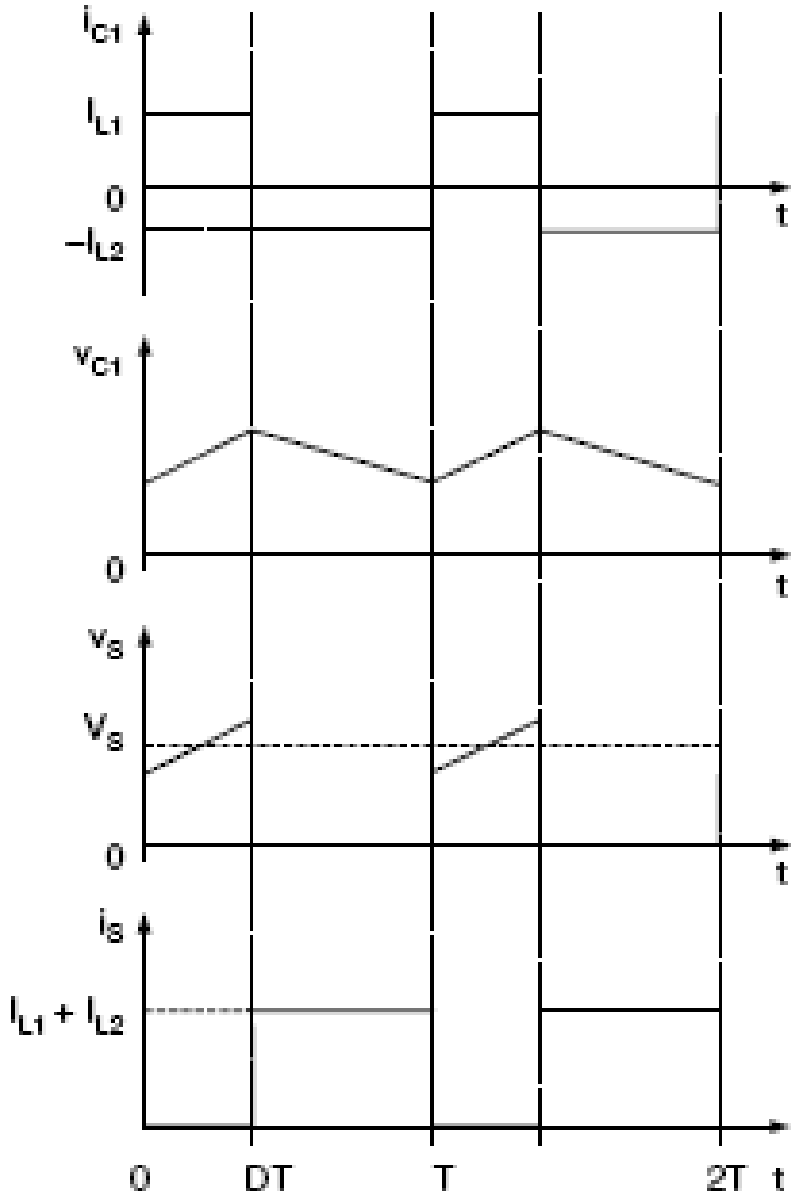


Figure 4.2: Waveforms of Cuk Converter

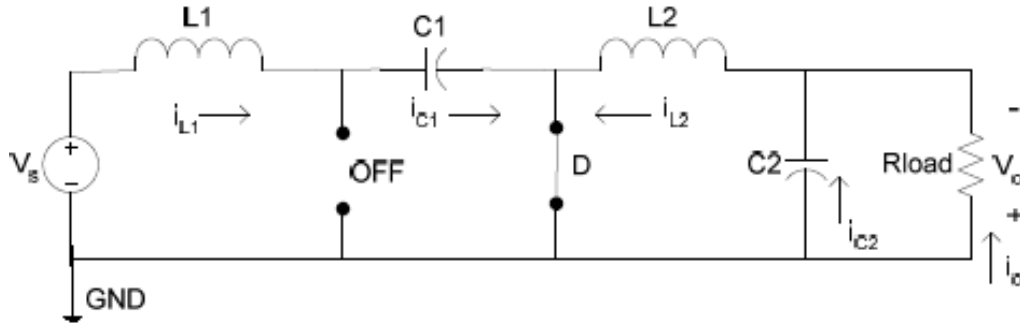


Figure 4.3: Cuk Converter when the switch is ON

circuit can be divided into two modes.

- Mode 1: When SW turns ON, the circuit becomes one shown in Figure 4-3.

The voltage of the capacitor (C_1) makes the diode (D) reverse-biased and turned off. The capacitor (C_1) discharge its energy to the load through the loop formed with SW, C_2 , R load, and L_2 . The inductors are large enough, so assume that their currents are ripple free. Thus, the following relationship is established.

$$-I_{C1} = I_{L2} \quad (4.5)$$

- Mode 2: When SW turns OFF, the circuit becomes one shown in Figure 4.4.

The capacitor (C_1) is getting charged by the input (V_s) through the inductor (L_1). The energy stored in the inductor (L_2) is transfer to the load through the loop formed by D, C_2 , and R load. Thus, the following relationship is established.

$$I_{C1} = I_{L1} \quad (4.6)$$

For periodic operation, the average capacitor current is zero. Thus, from the equation (2.5) and (2.6)

$$[I_{C1SW_{ON}}]DT + [I_{C2SW_{OFF}}](1 - D)T = 0 \quad (4.7)$$

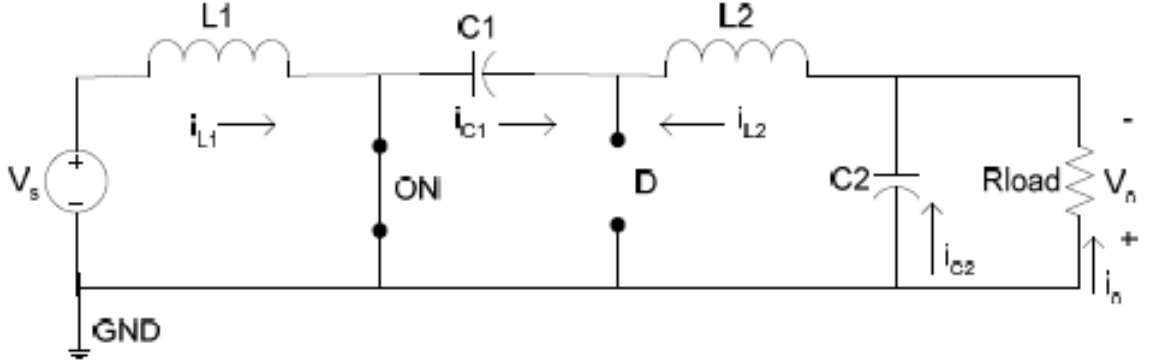


Figure 4.4: Cuk Converter when the switch is OFF

$$- I_{L2}DT + I_{L1}(1 - D)T = 0 \quad (4.8)$$

$$\frac{I_{L1}}{I_{L2}} = \frac{D}{1 - D} \quad (4.9)$$

where: D is the duty cycle ($0 < D < 1$), and T is the switching period. Assuming that this is an ideal converter, the average power supplied by the source must be the same as the average power absorbed by the load.

$$P_{in} = P_{out} \quad (4.10)$$

$$V_s I_{L1} = V_o I_{L2} \quad (4.11)$$

$$\frac{I_{L1}}{I_{L2}} = \frac{V_o}{V_s} \quad (4.12)$$

Combining the equation (4.9) and (4.12), the following voltage transfer function is derived

$$\frac{V_o}{V_s} = \frac{D}{1 - D} \quad (4.13)$$

Its relationship to the duty cycle (D) is:

- If $0 < D < 0.5$ the output is smaller than the input.

- If $D = 0.5$ the output is the same as the input.
- If $0.5 < D < 1$ the output is larger than the input.

4.3 Mechanism of Load Matching

As described in Section 3.1, when PV is directly coupled with a load, the operating point of PV is dictated by the load (or impedance to be specific). The impedance of load is described as below.[7]

$$R_{load} = \frac{V_o}{I_o} \quad (4.14)$$

where: V_o is the output voltage, I_o is the output current. The optimal load for PV is described as:

$$R_{opt} = \frac{V_{MPP}}{I_{MPP}} \quad (4.15)$$

where: V_{MPP} and I_{MPP} are the voltage and current at the MPP respectively. When the value of R_{load} matches with that of R_{opt} , the maximum power transfer from PV to the load will occur. These two are, however, independent and rarely matches in practice. The goal of the MPPT is to match the impedance of load to the optimal impedance of PV. The following is an example of load matching using an ideal (lossless) Ck converter. From the equation (4.13):

$$V_s = \frac{1-D}{D} \cdot V_o \quad (4.16)$$

From the equation (4.12):

$$\frac{I_s}{I_o} = \frac{I_{L1}}{I_{L2}} = \frac{V_o}{V_s} \quad (4.17)$$

From the equations (4.16) and (4.17):

$$I_s = \frac{D}{1-D} \cdot I_o \quad (4.18)$$

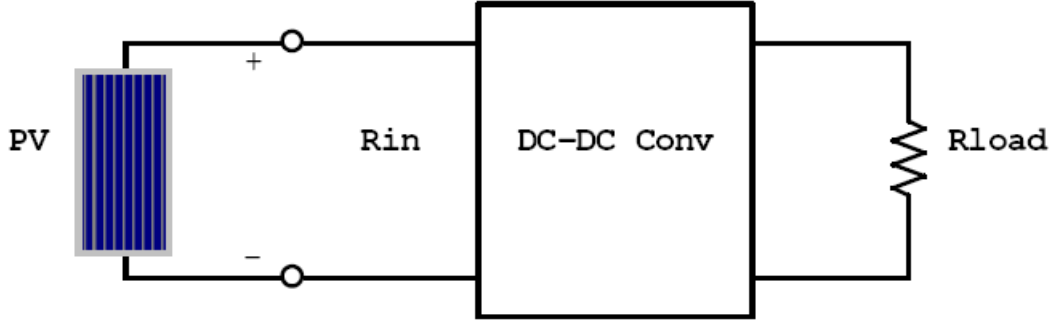


Figure 4.5: The impedance seen by PV is R_{in} that is adjustable by duty cycle (D)

From the equations (4.16) and (4.18), the input impedance of the converter is:

$$R_{in} = \frac{V_s}{I_s} = \frac{(1-D)^2}{D^2} \cdot \frac{V_o}{I_o} = \frac{(1-D)^2}{D^2} \cdot R_{load} \quad (4.19)$$

As shown in Figure 4.5, the impedance seen by PV is the input impedance of the converter (R_{in}). By changing the duty cycle (D), the value of R_{in} can be matched with that of R_{opt} . Therefore, the impedance of the load can be anything as long as the duty cycle is adjusted accordingly.

The main drawback of MPPT is that there is no regulation on output while it is tracking a maximum power point. It cannot regulate both input and output at the same time. The example of load matching in above is elaborated here to show how the output voltage and current change with varying irradiation. The maximum power transfer occurs when the input impedance of converter matches with the optimal impedance of PV module, as described in the equation below.

$$R_{in} = R_{opt} = \frac{V_{MPP}}{I_{MPP}} \quad (4.20)$$

The equation 4.19 is solved for duty cycle(D).

$$D = \frac{1}{1 + \sqrt{\frac{R_{in}}{R_{load}}}} \quad (4.21)$$

PV Module				MPPT				
Irradiance (W/m ²)	V _{MPP} (V)	I _{MPP} (A)	P _{max} (W)	R _{in} (Ω)	D	V _o (V)	I _o (A)	P _o (W)
1000	17.5	4.57	80.05	3.8	0.5568	21.98	3.63	79.8
800	17.06	3.73	63.6	4.57	0.5339	19.54	3.25	63.5
600	17.02	2.79	47.48	6.1	0.4979	16.87	2.81	47.4
400	16.81	1.86	31.26	9.03	0.4490	13.69	2.28	31.2
200	16.32	0.93	15.17	17.54	0.3690	9.54	1.59	15.16

Table I: Load matching with resistive load (6Ω) under the varying irradiance

PV Module				MPPT				
Irradiance (W/m ²)	V _{MPP} (V)	I _{MPP} (A)	P _{max} (W)	R _{in} (Ω)	D	V _o (V)	I _o (A)	P _o (W)
1000	17.5	4.57	80.05	3.8	0.6399	31.09	2.57	79.9
800	17.06	3.73	63.6	4.57	0.6183	27.63	2.30	63.55
600	17.02	2.79	47.48	6.1	0.5837	23.86	1.90	47.48
400	16.81	1.86	31.26	9.03	0.5354	19.37	1.61	31.18
200	16.32	0.93	15.17	17.54	0.4526	13.49	1.12	15.1

Table II: Load matching with resistive load (12Ω) under the varying irradiance

From the equation 4.13, the output voltage of the converter is:

$$V_o = \frac{D}{(1-D)} \cdot V_s \quad (4.22)$$

From the equation 4.18, the output current of the converter is:

$$I_o = \frac{(1-D)}{D} \cdot I_s \quad (4.23)$$

The calculation results are tabulated in the tables below. PV module data are obtained from the simulation model. Using the equations above, two sets of data are collected for the resistive load of 6Ω and 12Ω at the constant module temperature of 25°C.

Chapter 5

The Proposed System

Photovoltaic (PV) generators are increasingly being used in many remote area applications. It is important to extract maximum power from PV under varying temperature and solar radiation levels. A maximum power point tracking (MPPT) device is used between the PV array and the load (typically batteries) to optimize the power transfer from the PV array to the load. Since efficiency is a critical issue in small scale photovoltaic systems, power electronic converters used for this purpose are supposed to have very high efficiency. Techniques proposed to improve the converter efficiency by reducing switching loss using the zero current/voltage switching method, integrating PV modules with the converter system, reducing the PV module temperature and introducing new topologies for the converter have been reported. Controlling the power flow by providing two paths using a parallel power transfer (PPT) technique results in reduced power loss in the converter. The parallel power transfer approach is to split the power flowing into the load into two paths as: (1) power flowing directly to the load without the converter (P_p) and (2) power flowing to the load through the converter (P_m). This is shown in Fig.5.1[8]

As shown in Figure 5.2, the system is very simple and consists of a single PV module, a maximum power point tracker (MPPT), and a battery. The size of the system is intended to be small; therefore it could be built in the lab in the future. The system including the subsystems will be simulated to verify the functionalities.

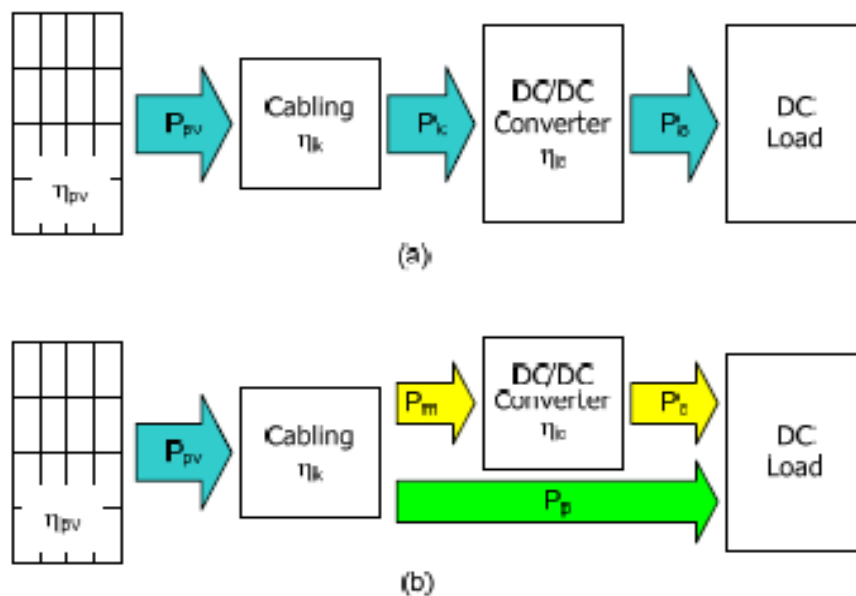


Figure 5.1: Power flow of converter in (a) conventional and (b) PPT configuration.

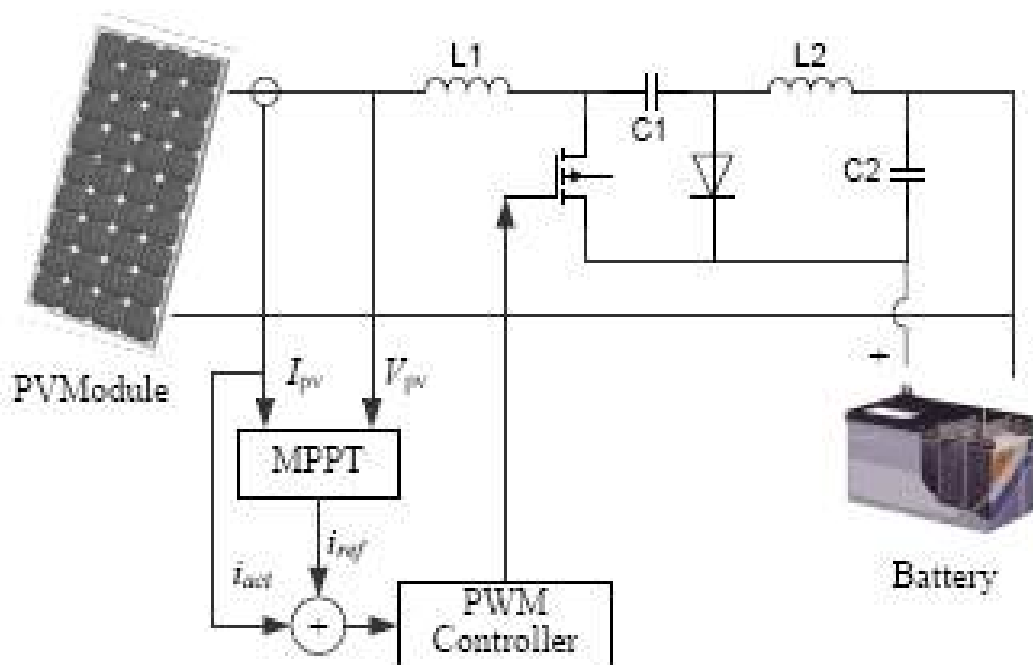


Figure 5.2: Cuk converter in PPT configuration for solar charge controller application.

Chapter 6

Design and Simulations

6.1 Introduction

This chapter provides the design and simulations of MPPT. It discusses Cuk converter design. After the component selection, simulations perform comparative tests of the P&O and Incremental Conductance algorithm. Simulations also verify the functionality of MPPT with a resistive load.

6.2 Cuk Converter Design

The basic operation of Cuk Converter and derivation of the voltage transfer function is explained in Section 4.2. Here, a Cuk converter is designed based on the calculations. After component selection, the design is simulated.[8]

- Rated input voltage $V_s = 17.5$ V
- Rated output voltage $V_o = 12$ V
- Rated input power $P_s = 80$ W
- Switching frequency $f = 50$ kHz

Design specification listed above leads the steady state parameters of the converter to operating points as follow:

$$D = \frac{V_o}{V_s} = \frac{12}{17.5} = 0.6857 \quad (6.1)$$

$$I_1 = \frac{P_s}{V_s} = \frac{80}{17.5} = 4.5714A \quad (6.2)$$

$$I_2 = \frac{D'}{D}(I_1) = \frac{1 - 0.6857}{0.6857}(4.5714) = 2.0619A \quad (6.3)$$

$$R_2 = \frac{V_o}{I_1 + I_2} = \frac{12}{4.5714 + 2.0619} = 5.4\Omega \quad (6.4)$$

6.2.1 Calculations

The inductor sizes are decided such that the change in inductor currents is no more than 10% of the average inductor current. The following equation gives the change in inductor current:[9]

$$\Delta i_l = \frac{V_s \cdot D}{L \cdot f} \quad (6.5)$$

where: V_s is the input voltage, D is the duty cycle, and f is the switching frequency. Solving this for L gives:

$$L = \frac{V_s \cdot D}{\Delta i_l \cdot f} \quad (6.6)$$

Assume that the worst current ripple will occur under the maximum power condition. Under this condition, the average current (I_{L_1}) of the input inductor (L_1) is 4.5A, and the ripple current is 10% of I_{L_1} .

$$\Delta i_{L_1} = 0.1 \cdot I_{L_1} = (0.1) \cdot (4.5714) = 0.45714A \quad (6.7)$$

Thus, from equation 6.6:

$$L_1 \geq \frac{V_s \cdot D}{\Delta i_{L_1} \cdot f} = \frac{(17.5)(0.6857)}{(0.45714)(50 \times 10^3)} \geq 525\mu H \quad (6.8)$$

Similarly, the value of the output inductor (L_2) is calculated as follows:

$$\Delta i_{L_2} = 0.1 \cdot I_{L_2} = (0.1) \cdot (2.0619) = 0.2062A \quad (6.9)$$

$$L_2 \geq \frac{V_s \cdot D}{\Delta i_{L_2} \cdot f} = \frac{(17.5)(0.6857)}{(0.2062)(50 \times 10^3)} \geq 1.16mH \quad (6.10)$$

The design criterion for capacitors is that the ripple voltage across them should be less than 10%. The average voltage across the capacitor (C_1) is, from the equation (4.4), $V_{C_1} = V_s + V_o = 17.5 + 12 = 30V$. So the maximum ripple voltage is $\Delta v_{C_1} = 0.1 \times 30 = 3V$. The equivalent load resistance is:

$$R = \frac{V_o^2}{P_o} = \frac{12^2}{80} = 1.8\Omega \quad (6.11)$$

The value of C_1 is calculated with the following equation:

$$C_1 = \frac{V_o \cdot D}{R \cdot f \cdot \Delta v_{C_1}} = \frac{(12 \times 0.6857)}{(1.8 \times 50 \times 10^3 \times 3)} = 30.47\mu F \quad (6.12)$$

The value of the output capacitor (C_2) is calculated using the output voltage ripple equation (the same as that of buck converter):

$$\frac{\Delta v_o}{V_o} = \frac{(1 - D)}{8 \cdot L_2 \cdot C_2 \cdot f^2} \quad (6.13)$$

Solving the above equation for C_2 gives:

$$C_2 = \frac{(1 - D)}{8 \cdot \left(\frac{\Delta v_o}{V_o}\right) \cdot L_2 \cdot f^2} = \frac{(1 - 0.6857)}{8 \times 0.1 \times 1.16 \times 10^{-3} \times (50 \times 10^3)^2} = 0.1354\mu F \quad (6.14)$$

The circuit of a Cuk converter in PPT configuration is presented in figure 6.1. Input and output equation in state space presentation of the inductor voltages and capacitor currents is written as

$$\bar{x} = \bar{A}\bar{x}(t) + \bar{B}\bar{u}(t) \quad (6.15)$$

$$\bar{y} = \bar{C}\bar{x}(t) + \bar{E}\bar{u}(t) \quad (6.16)$$

$$\bar{\dot{x}} = \begin{bmatrix} 0 & \frac{-D'}{L_1} & 0 & \frac{-1}{L_1} \\ \frac{D'}{C_1} & 0 & \frac{-D}{C_1} & 0 \\ 0 & \frac{D}{L_2} & 0 & \frac{-1}{L_2} \\ \frac{1}{C_2} & 0 & \frac{1}{C_2} & \frac{-1}{RC_2} \end{bmatrix} \begin{bmatrix} i_1(t) \\ v_1(t) \\ i_2(t) \\ v_2(t) \end{bmatrix} + \begin{bmatrix} \frac{V_1}{L_1} \\ \frac{-(I_1+I_2)}{C_1} \\ \frac{V_1}{L_2} \\ 0 \end{bmatrix} d(t) \quad (6.17)$$

$$\bar{y} = \begin{bmatrix} 1 & 0 & 0 & 0 \end{bmatrix} \begin{bmatrix} i_1(t) \\ v_1(t) \\ i_2(t) \\ v_2(t) \end{bmatrix} \quad (6.18)$$

Substituting the steady state operating parameters of the Cuk converter into equation yields a transfer function of power stage.

$$T_p(s) = \frac{33.22 \times 10^3 s^3 + 3.9 \times 10^9 s^2 + 1.26 \times 10^{13} s + 4.9 \times 10^{16}}{s^4 + 118.2 \times 10^3 s^2 + 217.22 \times 10^6 s^2 + 5.46 \times 10^{11} s + 1.02 \times 10^{15}} \quad (6.19)$$

6.3 Simulation and Results

The Simulation model of the PV-module is shown in Figure 6.1. The input of PV-module block is V_1 (PV voltage), Suns (irradiation), and TaC (operating temperature). The output of the PV-module block is I (PV current) and P(PV Power). The PV-module uses the electrical parameter as listed in Equations 2.1,2.2 and 2.3 are adopted to model the I-V characteristics of the PV.[10]

The Simulation model of the overall system is shown in Figure 6.3. In the model, two PV modules are connected in series. The current output of the PV is fed to the cuk converter. MPPT block read the PV power and generate the corresponding duty cycle to the cuk converter.[11]

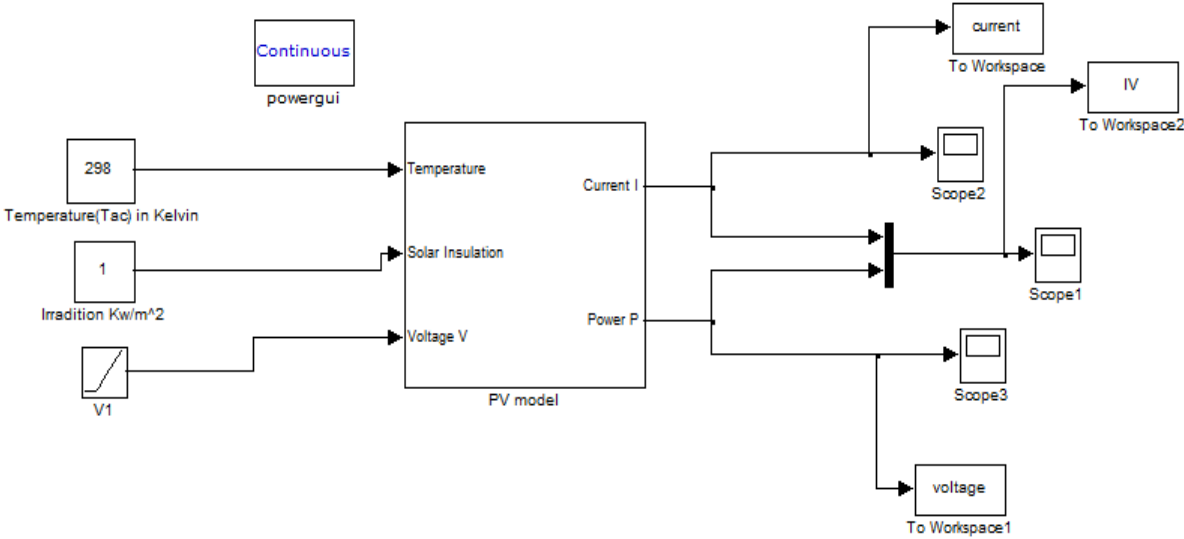


Figure 6.1: Simulation model of the PV module

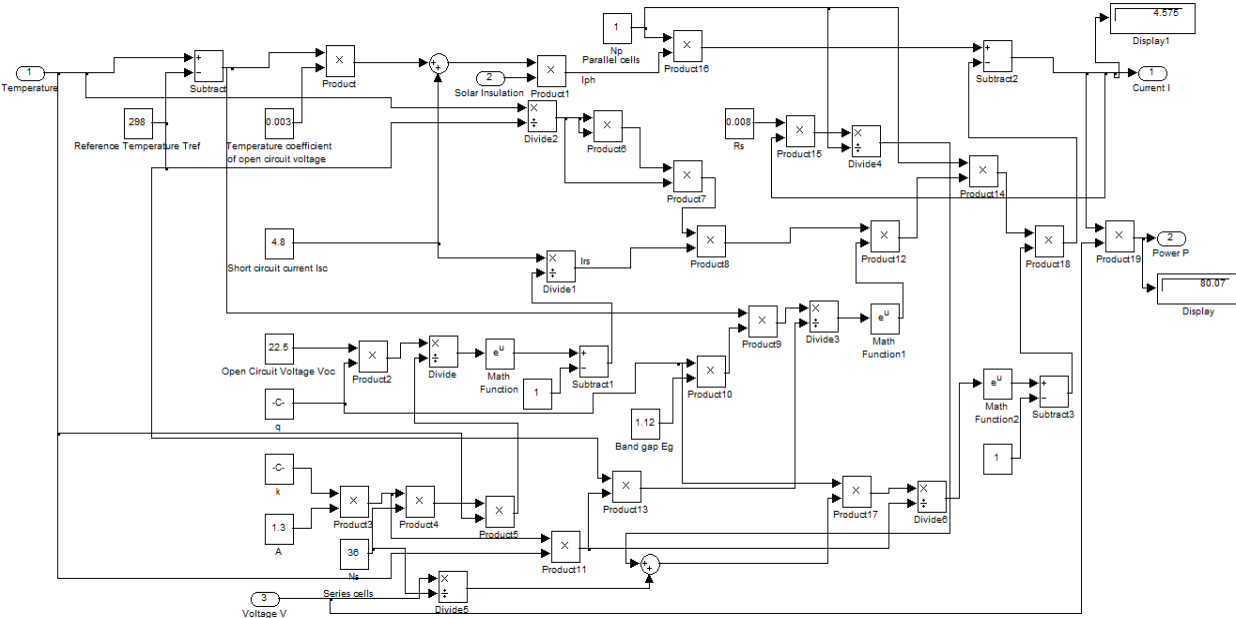


Figure 6.2: Subsystem of the PV module

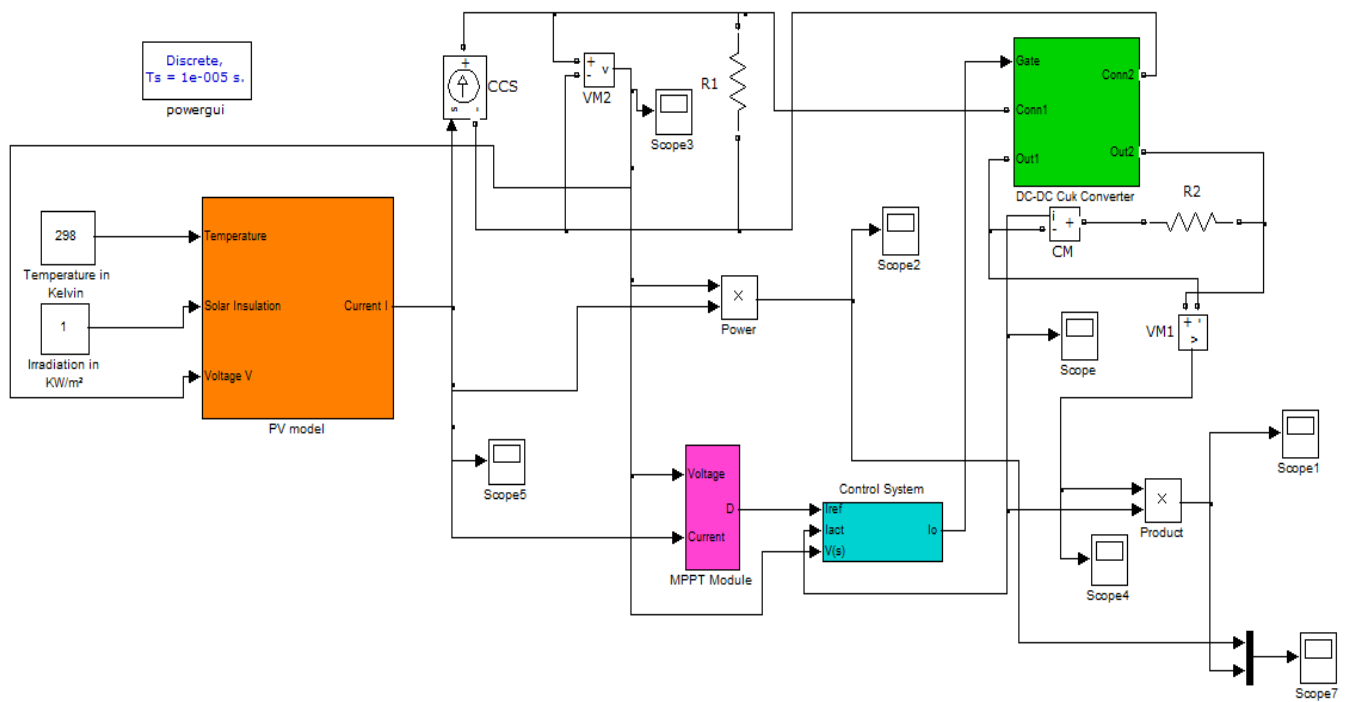


Figure 6.3: Simulink model of entire system with MPPT

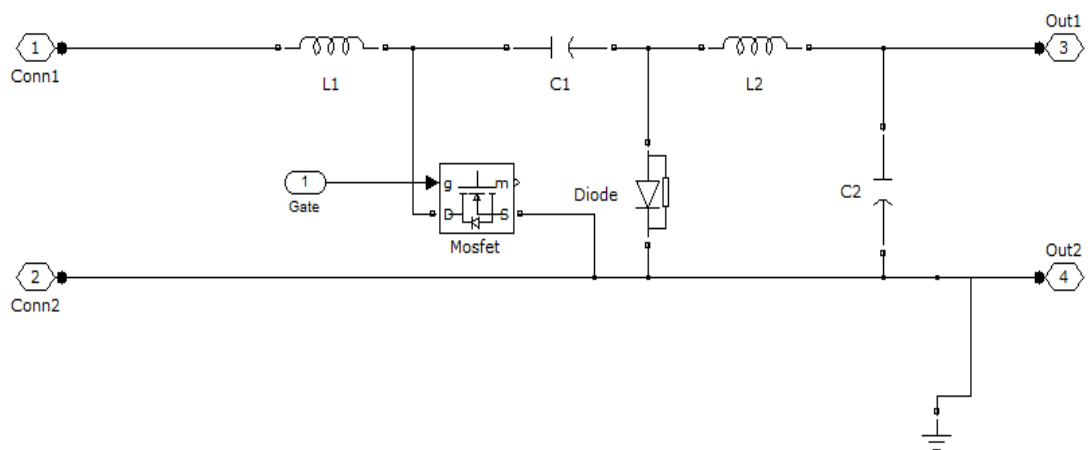


Figure 6.4: Subsystem of the cuk converter

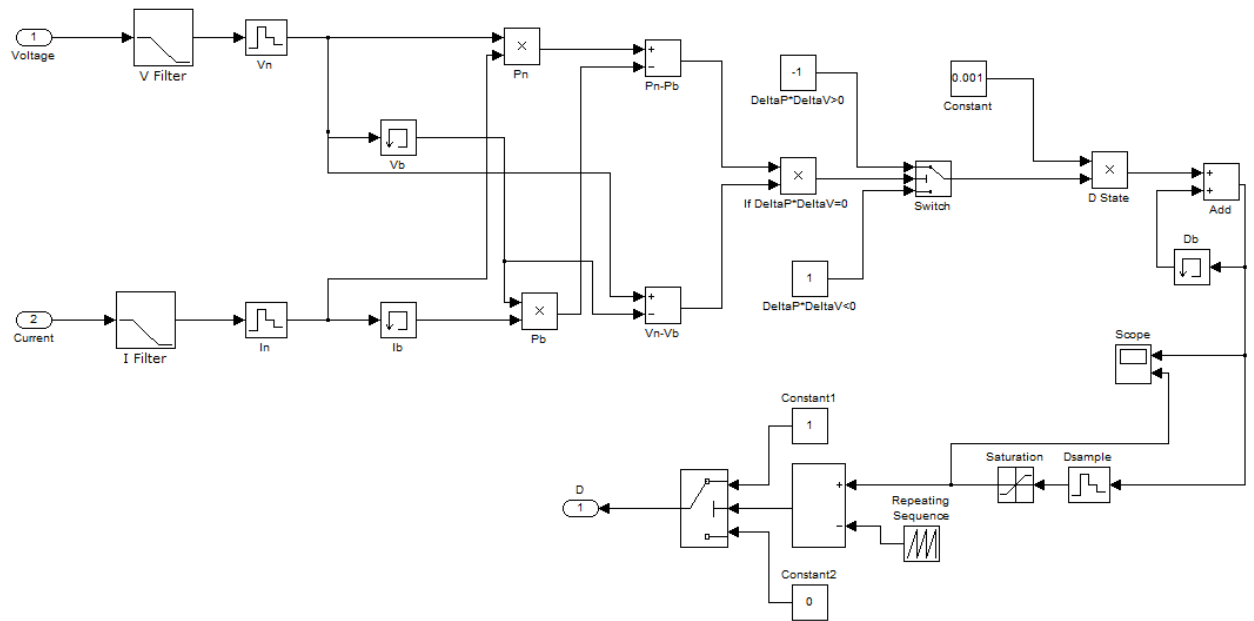


Figure 6.5: Subsystem of Incremental Conductance MPPT algorithm

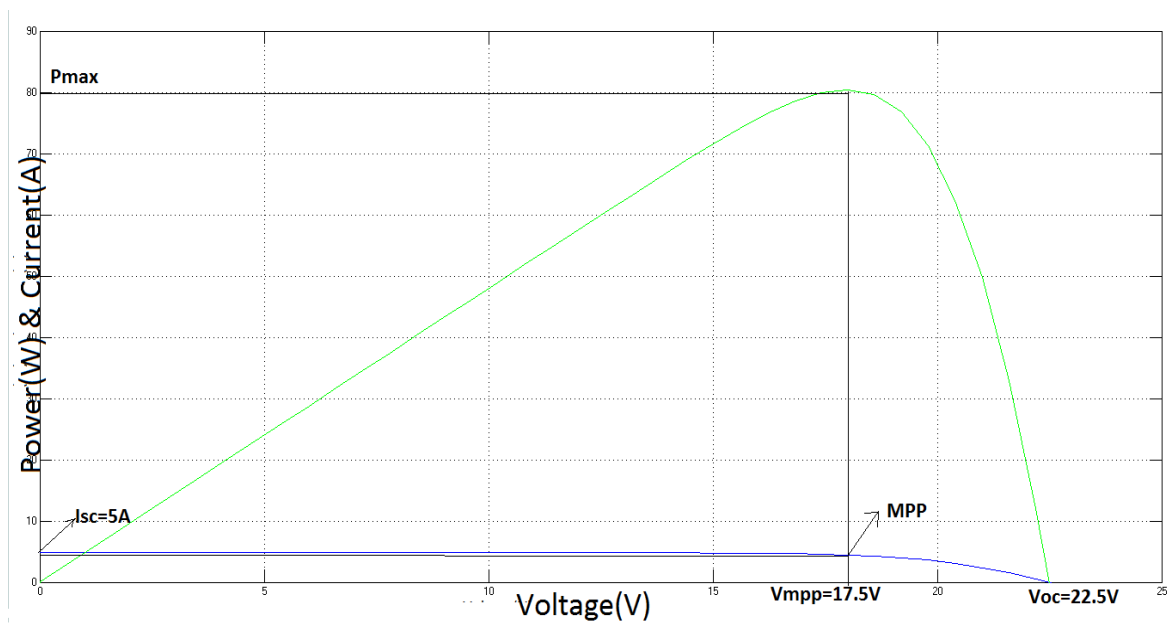


Figure 6.6: PV & IV curve of solar model

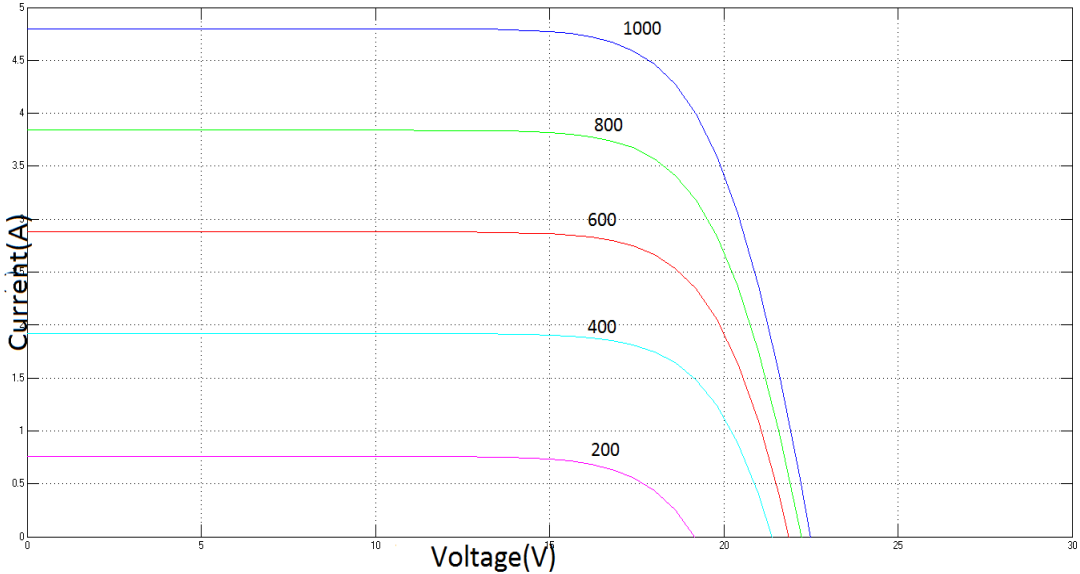


Figure 6.7: IV curves under different solar Irradiations(W/m²) at 25°C

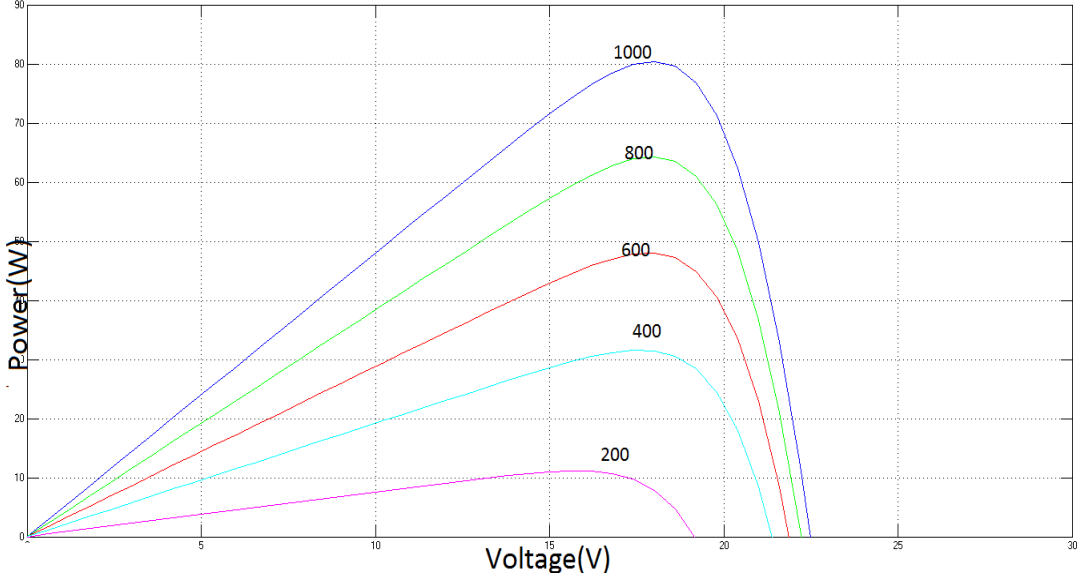


Figure 6.8: PV curves under different solar Irradiations(W/m²) at 25°C

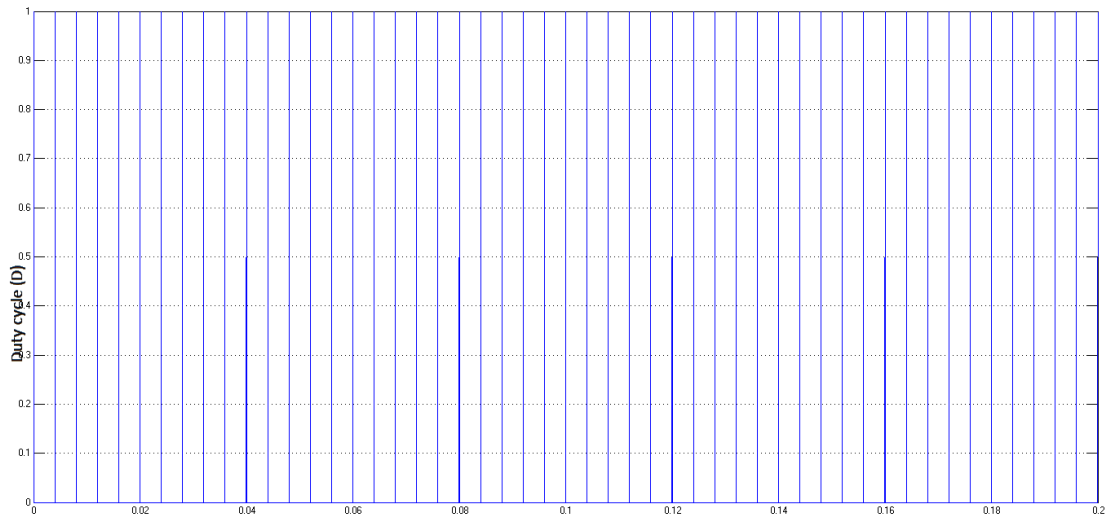
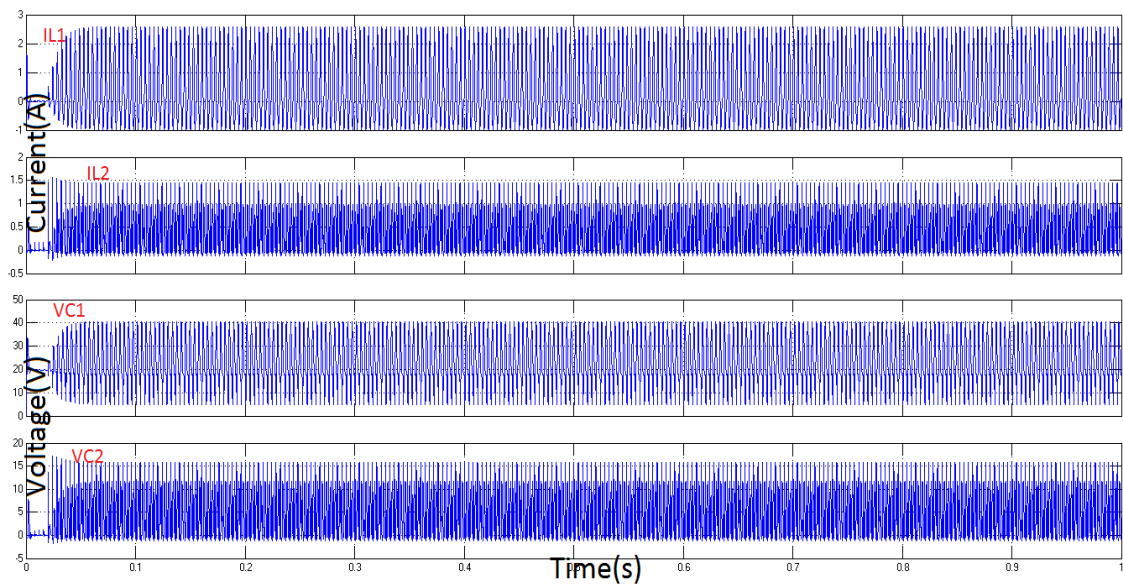


Figure 6.9: Gating signal from MPPT module

Figure 6.10: Voltage(V_{C1}, V_{C2}) & Current(I_{L1}, I_{L2}) of the Cuk Converter

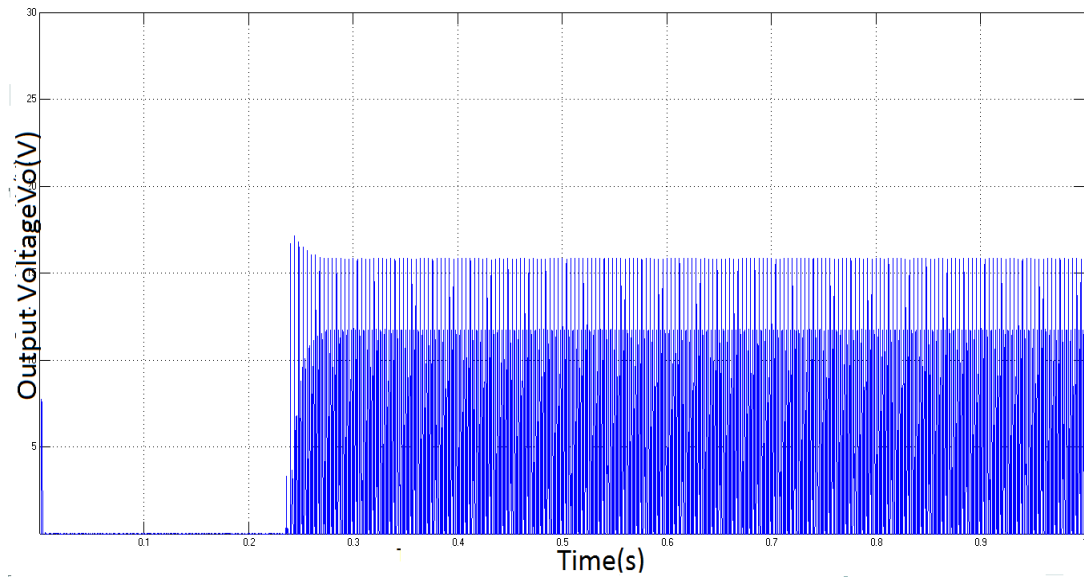


Figure 6.11: Output voltage of the Cuk Converter

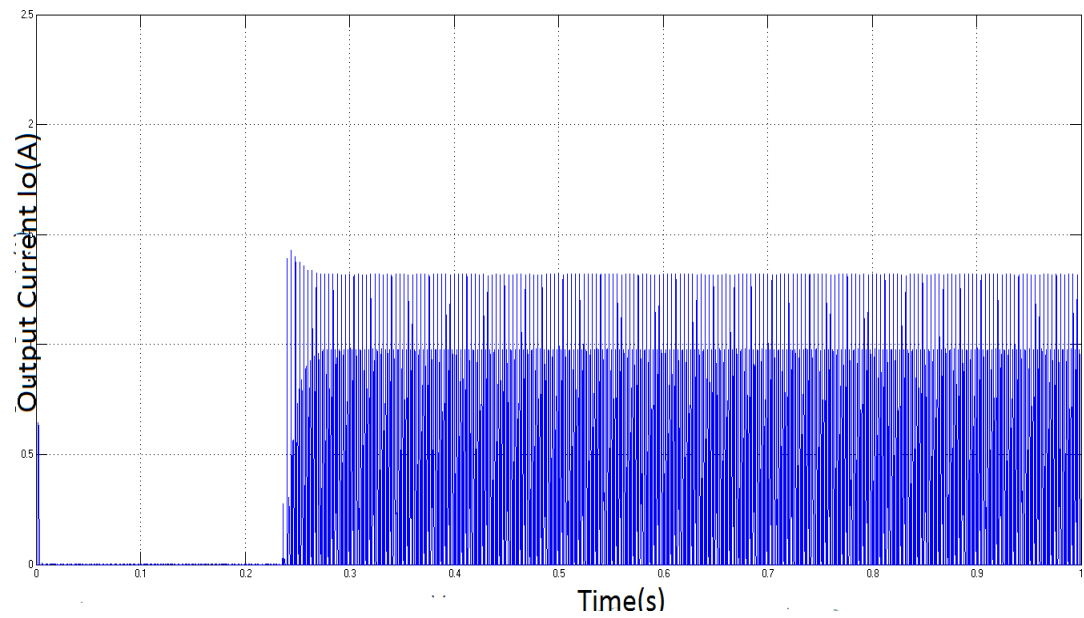


Figure 6.12: Output current of the Cuk Converter

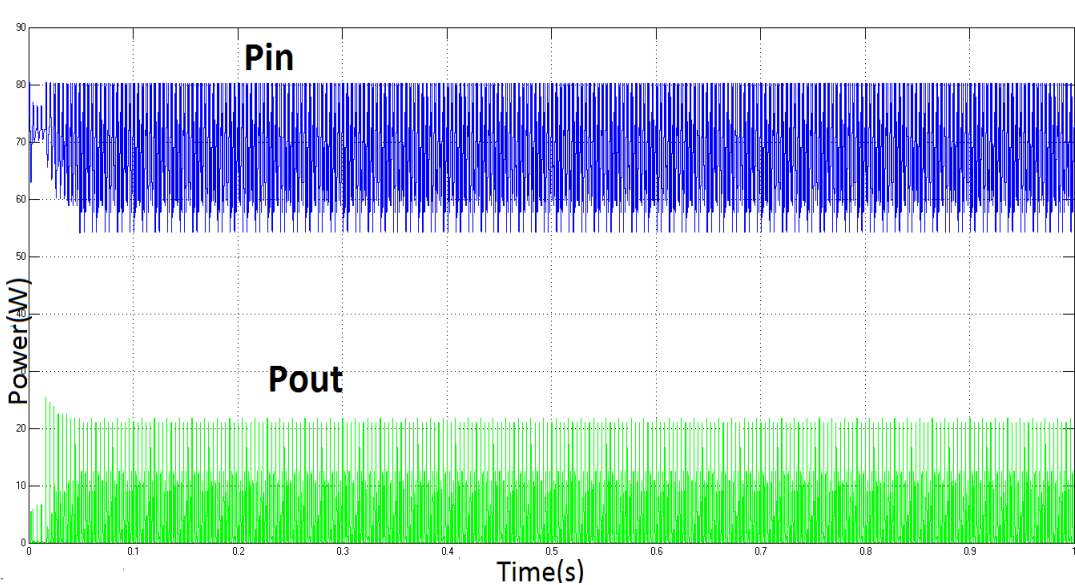


Figure 6.13: Comparison of the both powers Pin and Pout(without closed loop)

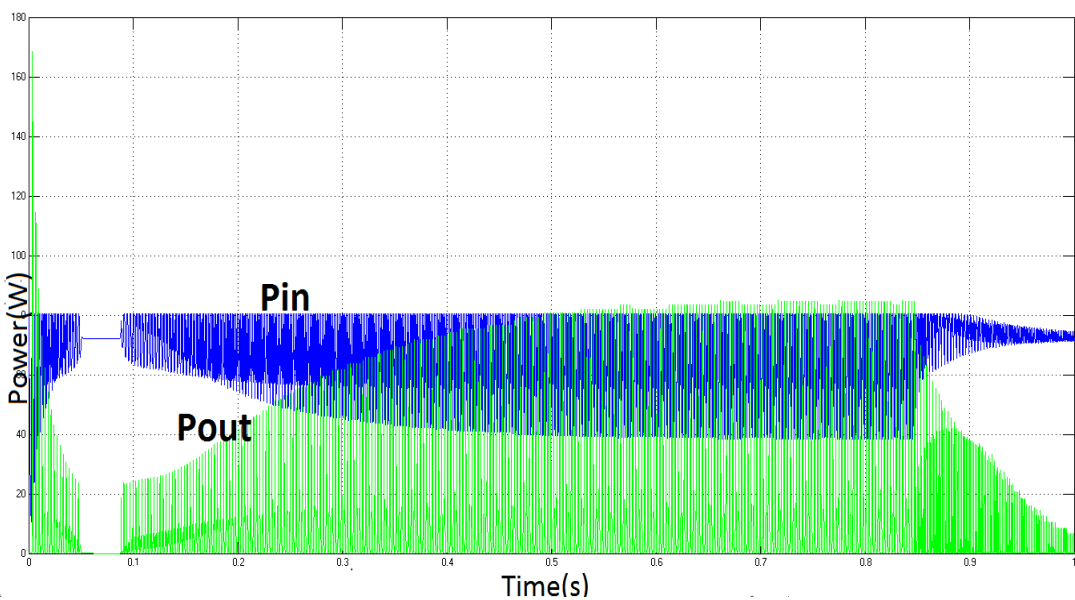


Figure 6.14: Comparison of the both powers Pin and Pout(with closed loop)

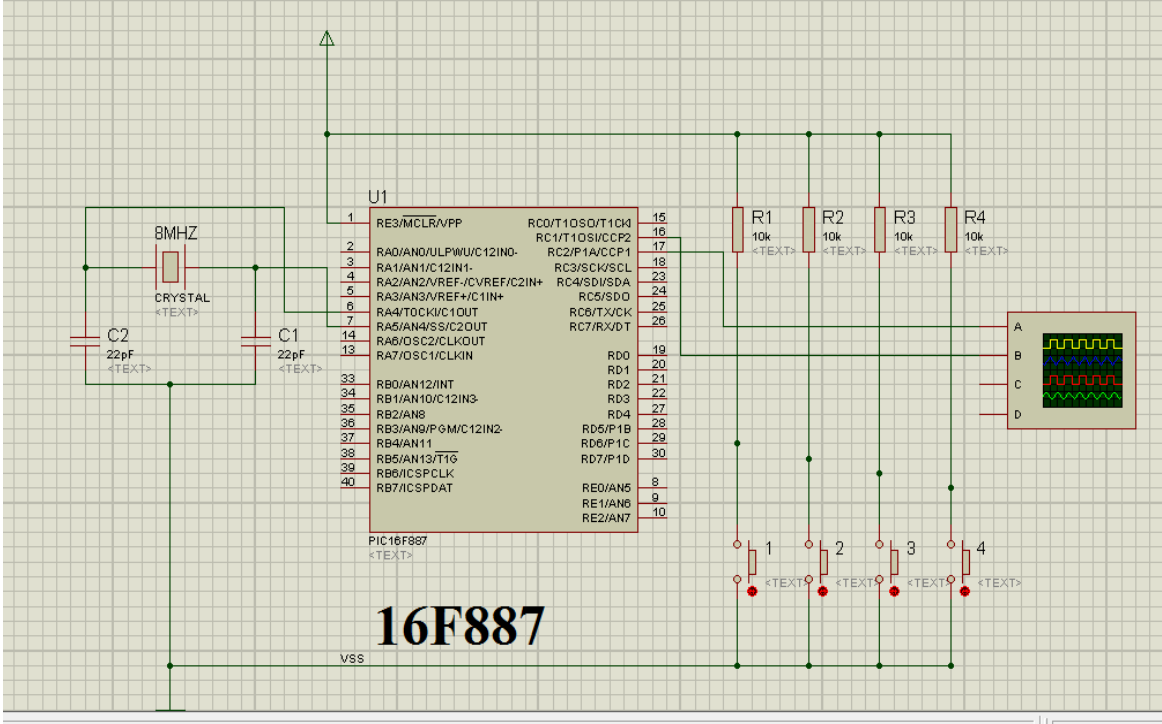


Figure 6.15: PIC simulation diagram

In order to use controller for MPPT algorithm, the MPPT code is build up in mikroC for PIC and hex file is saved. Then after PIC16F887 controller is encoded with MPPT code in Proteus software and result obtained is shown figure 6.15 & 6.16. Here 8MHz crystal frequency is connected across two 22pf capacitors. Supply is given accordingly and output is seen in oscilloscope.

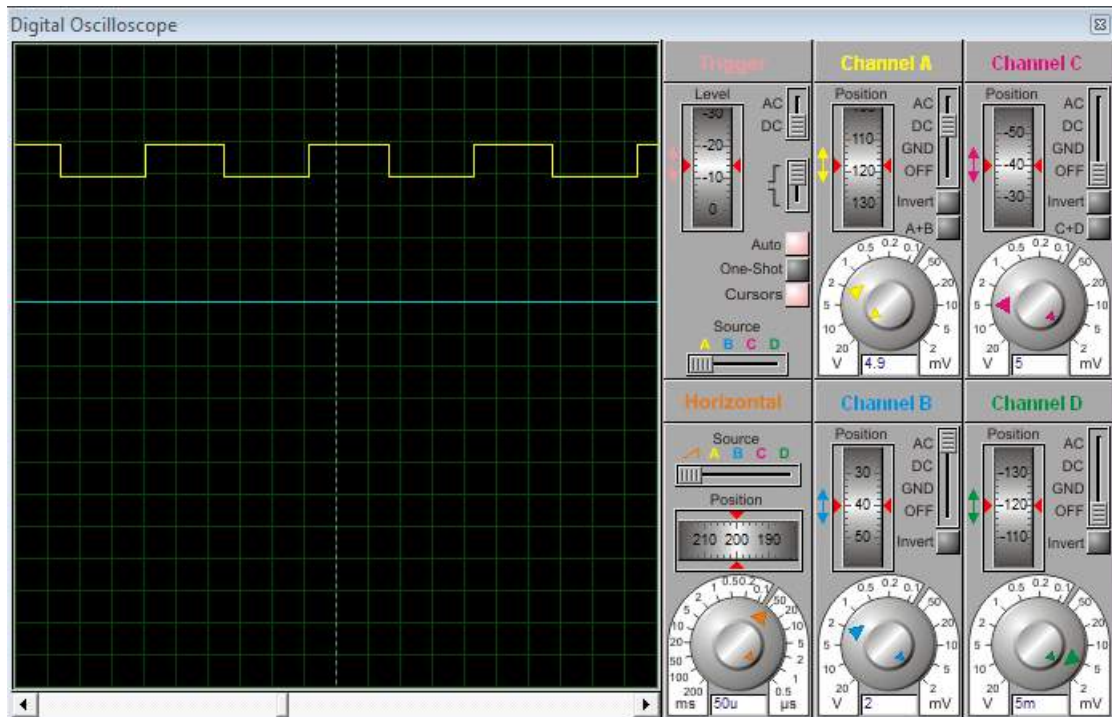


Figure 6.16: Pulses obtained from PIC controller

Chapter 7

Hardware Description

The practical implementation of cuk converter is made based on the simulation models earlier. The PV module has to be studied to understand the source response; hence its IV characteristics should be studied. Cuk converter module is designed based on the calculated values from the simulation. However, compatible ICs should be selected for ensuring proper operation of the converter. The resonant inductor and converter play a crucial role in operation and are designed using the inductor design equations and the capacitors are designed from the available standard values. The simulation model of feedback control of the error voltage (current mode control) is done to generate the duty cycle error for regulation of the output voltage. The overall block diagram of the solar power based charger is shown here.

7.1 Cuk Converter

Cuk Converter Circuit consists of MOSFETs, inductor, capacitors, diode and power supply. MOSFET used is IRF540N. It is a highly fast switching Integrated switch. Inductor is coiled around a ferrite core. The circuit is as built such that getting the desired set of switching pulse from the driving circuit; it steps down the voltage with lower switching loss by using soft switching techniques as mentioned before. The diode (1N4007) in the cuk converter is replaced with a Schottky diode as the forward

voltage drop is less in the Schottky diode and thus the power loss due to diode is also less.

7.1.1 MOSFET IRF540N

MOSFET used in the synchronous buck converter is IRF540N. It is an N-channel enhancement type power field effect transistor. IRF540N is a highly fast switching Integrated circuit. As the MOSFET can operate at high frequencies thus the output voltage is a steady DC voltage. The on- state drain to source resistance is very low for this MOSFET. Thus, the power loss due to the drain to source resistance is also very low. It also consists of an inherent body diode which helps in the operation of MOSFET in the reverse direction also. This body diode also helps in the operation of soft switching techniques in the cuk converter. Pin -1 Gate In this pin the gate pulse is input to the MOSFET. Pin -2 Drain In this pin the voltage VCC is supplied, which is positive with respect to the source. Pin -3 Source In this pin ground is connected through a load.

7.1.2 Schottky Diode

Schottky diode should be selected because it has a low forward voltage and very good reverse recovery time (typically 5 to 10ns). $V_{RRM} = 17.5+12= 30V$. Adding the 30% of safety factor gives the voltage rating of 39V. The average forward current (I_f) of diode is the combination of input and output currents at the SW off, thus it is $I_d = I_{L1}+I_{L2} = 4.5784+2.0619= 6.65A$. Adding the 30% of safety factor gives the current rating of 8.5A. Schottky diodes are widely available from numerous vendors. For example, MBR15100 ($I_f=15A_{max}$, $V_{RRM}=100V_{max}$) meets the above-mentioned voltage and current ratings.[7]

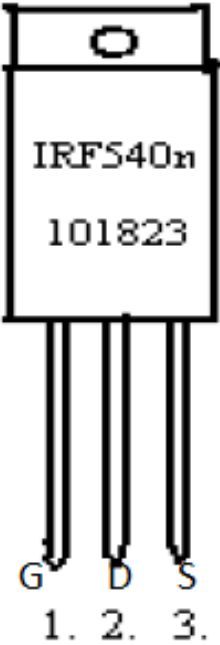


Figure 7.1: Pin configuration of IRF540N

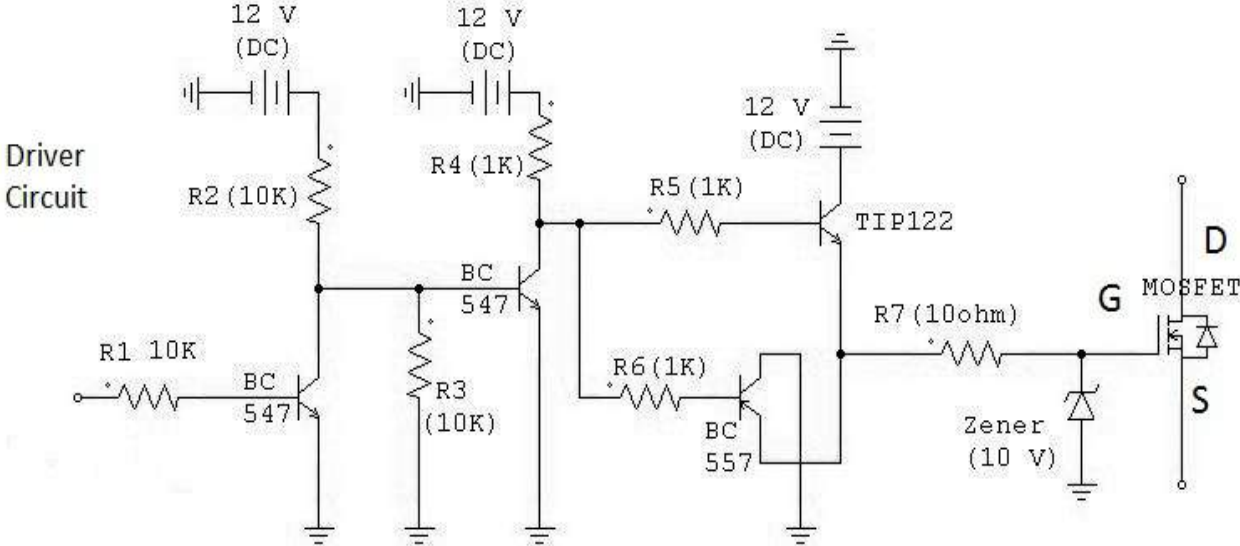


Figure 7.2: Driver circuit for MOSFET

Secondary terminals

- Terminal + : supply voltage + 15 V
- Terminal M: measure
- Terminal - : supply voltage - 15 V

Connection

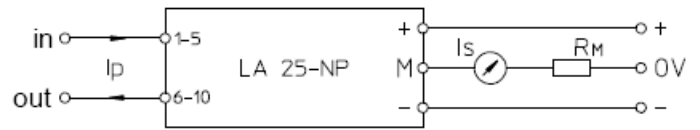


Figure 7.3: Pin diagram of LA25-NP

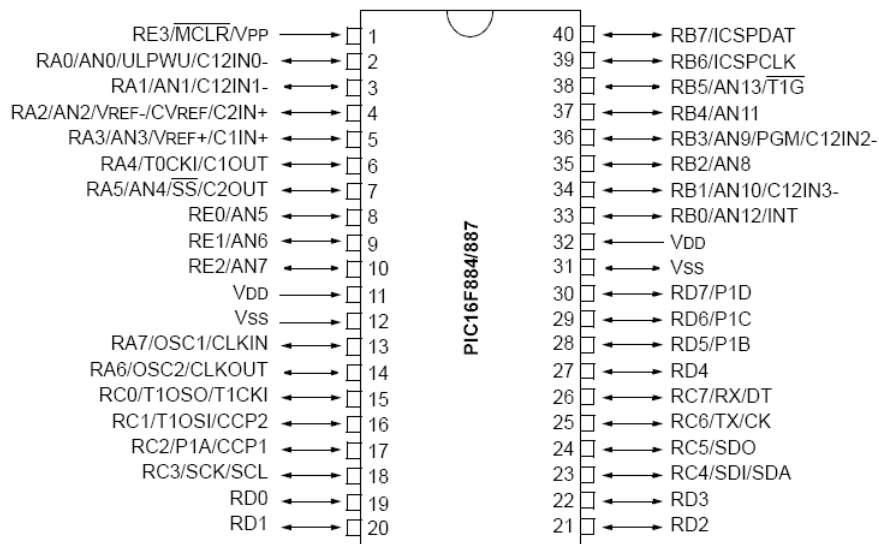


Figure 7.4: Pin configuration of PIC16F887

7.2 Control Circuit Configuration

In order to always exploit the maximum power from the PV module, the incremental conductance algorithm is coded into a PIC controller. The controller uses the input current and voltage of the converter to calculate the suitable PWM for the MOSFET. The PWM signal from the controller is amplified from 5V to 15V by using a gate drive circuit since the MOSFET operates with 12V signal. To sense the current from the solar panel LEM LA25-NP current sensor is used. The pin diagram is shown figure 7.3.

Here PIC16F887 from Microchip is used with used with frequency range between 8MHz to 31KHZ. The processing speed depends on the connection of the external clock generator circuit and the high speed crystal/resonator with phase-locked loop (PLL) enabled mode is used to produce the 40MHz clock pulse. A 8MHz crystal and two 10 pF capacitors are used to generate the clock pulse. Figure below shows the pin diagram of PIC16F887. And below that figure shows the hardware implementation of the PIC controller. Employing PIC controller has many advantages including cost efficiency of less than \$50, easy to programming and debugging, and large range of interfaces. They have also built-in oscillator with selectable speeds. They use 10-bit analog to digital converter (ADC) and processing speed of 40MHz which is appropriate for MPPT system. They can also provide the required frequency to generate the PWM signal. In summary, PIC is capable of taking control of the MPPT system with less cost and complexity compared to DSP.

Chapter 8

Experimental Results

The Whole setup is tested on 80W panel. LEM LA25-NP current sensor senses the current of the solar panel and two resistors 320Ω and 100Ω are connected in parallel for voltage divider. Voltage is measured across 100Ω and ground. The sensed current and voltage are given to PIC controller in which MPPT code is installed. Output of the PIC controller gives pulses of 50% duty cycle of 5V. The supply to the PIC controller is given through IC7805 which converts 12V to 5V. These pulses are given to the driver circuit which enhances the duty cycle and gives pulses of 10V. These driver circuit is given power supply through 12V SMPS. Then these pulses are given to the gate and source of the MOSFET so it turns on and converter starts working. The waveforms obtained when tested during sunny day are given in the figures:

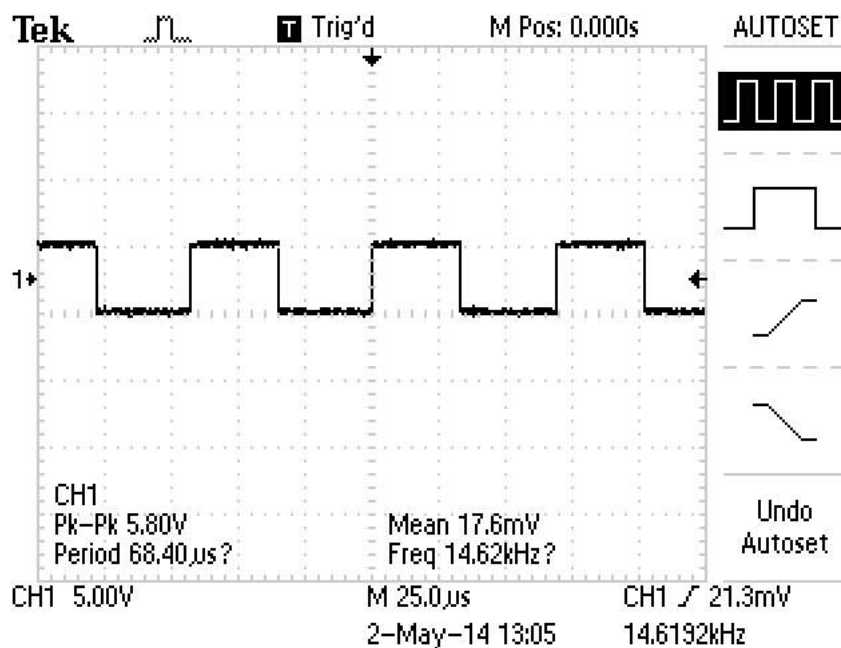


Figure 8.1: Pulses obtained from PIC controller [Scale: X-axis 1cm=25μs/div Y-axis 1cm=5V/div]

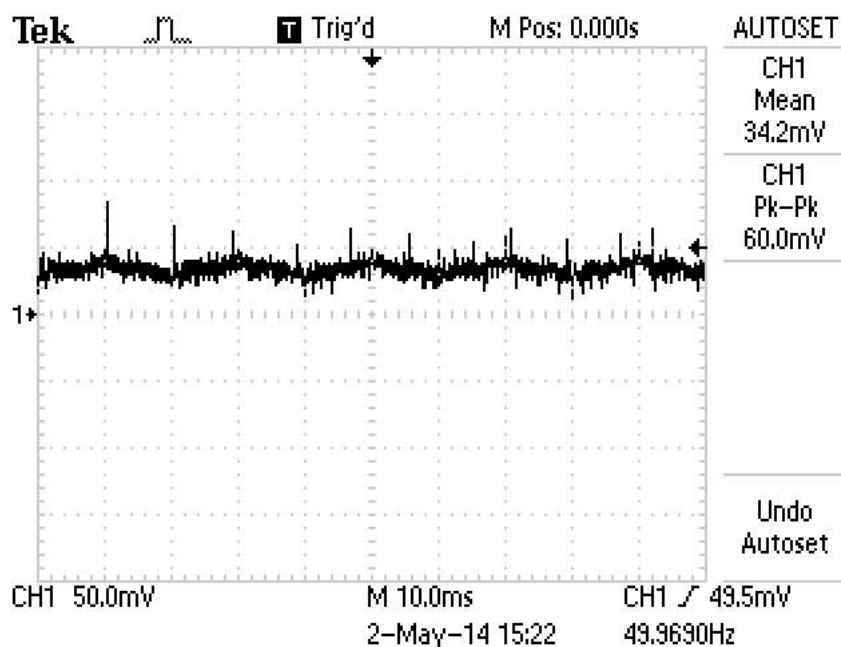


Figure 8.2: Solar Panel current sensed from LEM current sensor

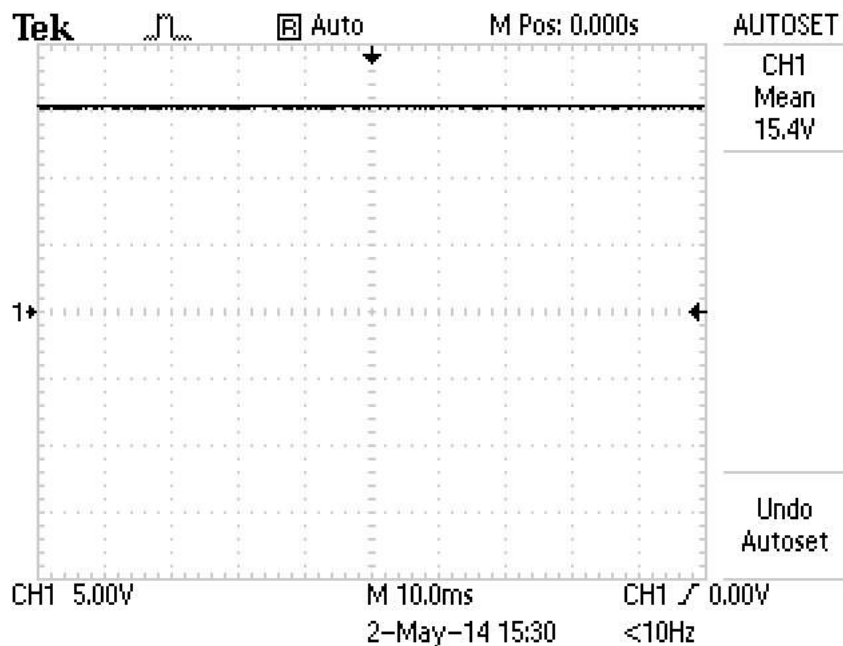


Figure 8.3: Solar Panel voltage

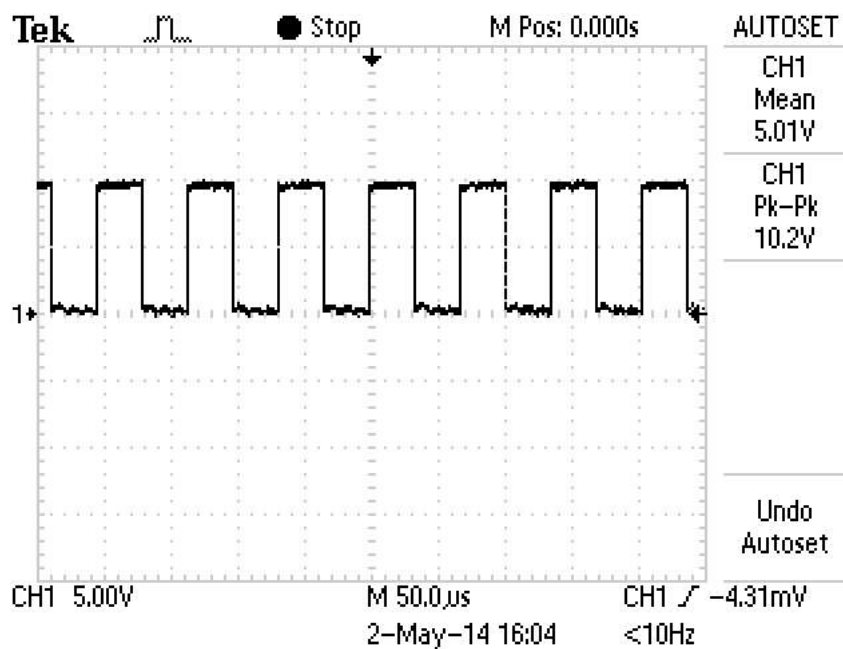


Figure 8.4: Pulses from the driver circuit [Scale:X-axis 1cm=50µs/div Y-axis 1cm=5V/div]

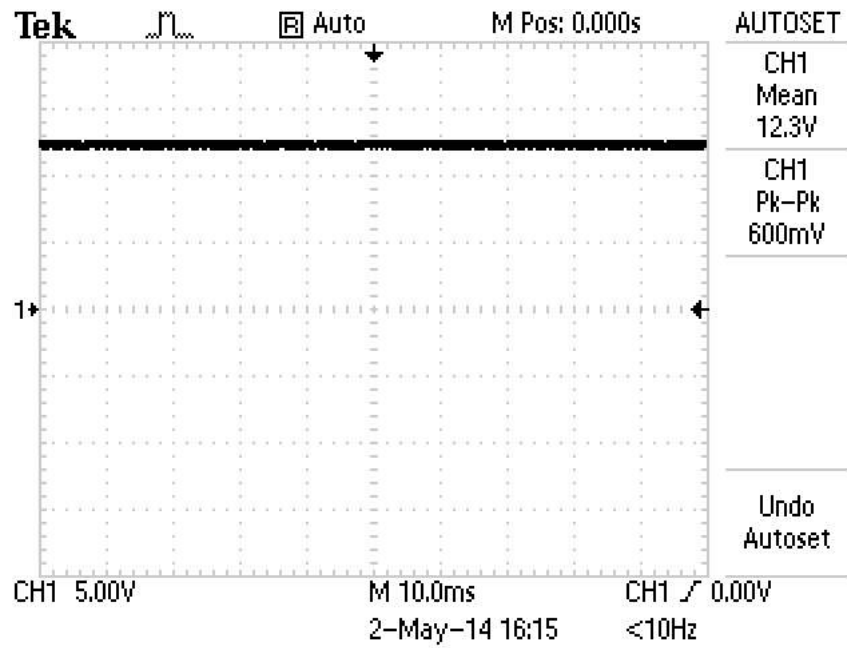


Figure 8.5: Output Voltage of the Cuk Converter

Chapter 9

Conclusion

9.1 Summary

The proposed MPPT system is able to track the MPP under constant and varying weather conditions. Therefore a low cost efficient MPPT system is designed, simulated and implemented. By using a low cost PIC controller to sense the PV module's output voltage and current, duty cycle of the Cuk converter is adjusted to keep the PV system operating at the MPP. Thus we obtained 12V output from Cuk Converter useful for battery charging applications.

9.2 Future Scope

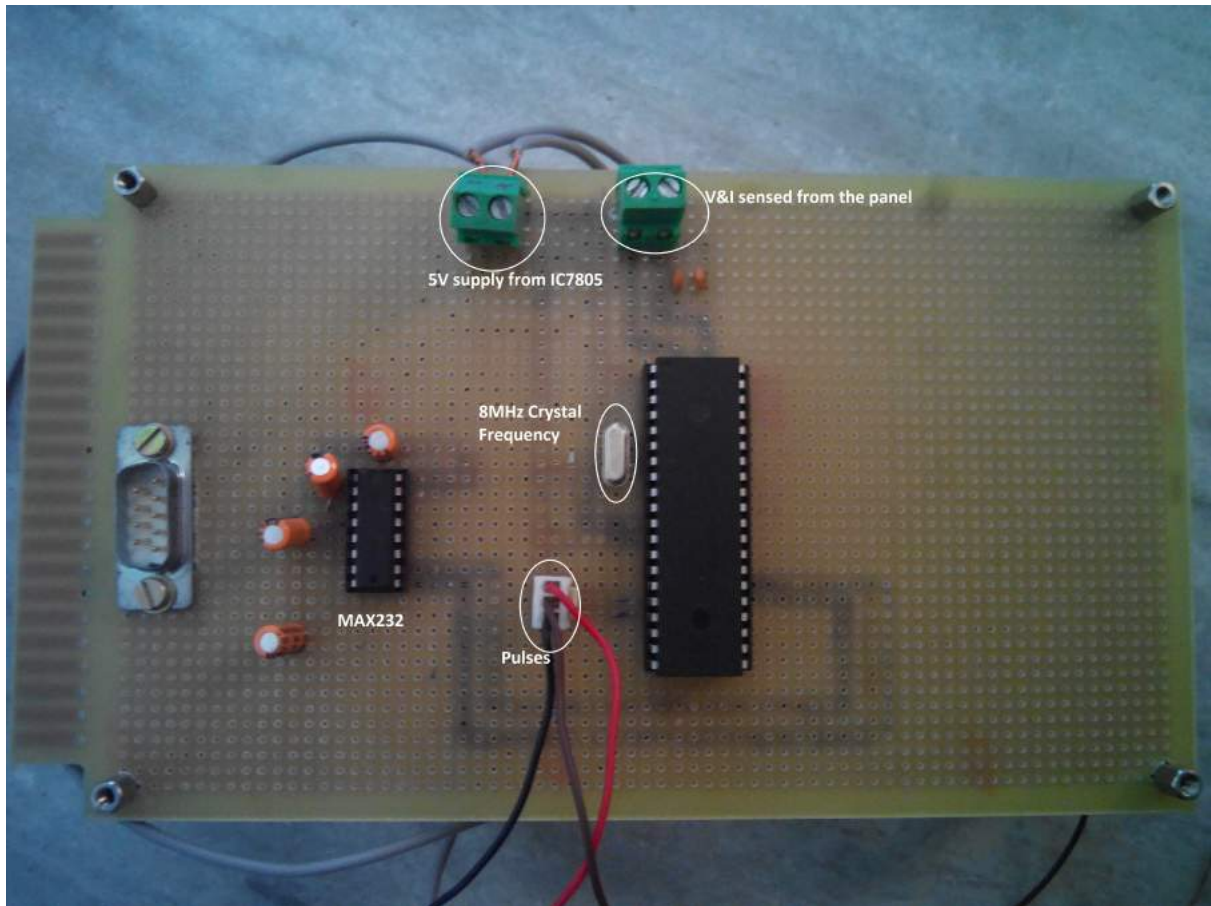
Improvement to this project can be made by tracking the maximum power point in changing environmental conditions. Environmental change can be change in solar irradiation or change in ambient temperature or even both. As an addition several data can be stored and analyzed to calculate the efficiency of MPPT and Cuk Converter. Furthermore it can be useful for multiphase Cuk Converter to get a higher output power and using load sharing control scheme we can improve the efficiency and power quality.

References

- [1] Power Electronics Handbook by M H Rashid/chapter 26-Solar Power Conversion
- [2] Power Electronics-Converters,Applications and Design by Ned Mohan,Tore M. Undeland and William P. Robbins/chapter no 7.DC-DC Switch Mode Converters
- [3] S.Sheik Mohammed, “Modeling and Simulation of Photovoltaic module using MATLAB/Simulink”, International Journal of Chemical and Environmental Engineering, Volume 2. October 2011.
- [4] Saurav Satpathy, “Photovoltaic Power Control Using Mppt And Boost Converter”, thesis submitted at Department of Electrical Engineering National Institute of Technology, Rourkela, May 2012.
- [5] Hairul Nissah Zainudin, Saad Mekhilef, Comparison Study of Maximum Power Point Tracker Techniques for PV Systems, Cairo University, Egypt, December 19-21, 2010, Paper ID 278.
- [6] Neeraj Tiwari, D. Bhagwan Das,“Mppt Controller For Photo Voltaic Systems Using Cuk Dc/Dc Converter”, International Journal of Advanced Technology & Engineering Research (IJATER), VOLUME 2, ISSUE 3, MAY 2012.
- [7] Akihiro Oi “Design and Simulation of Photovoltaic Water Pumping System” a thesis presented to the faculty of California Polytechnic State University.
- [8] D.C. Riawan, C.V. Nayar, “Analysis and design of a solar charge controller using Cuk Converter”, Power Engineering Conference, 2007, AUPEC 2007.

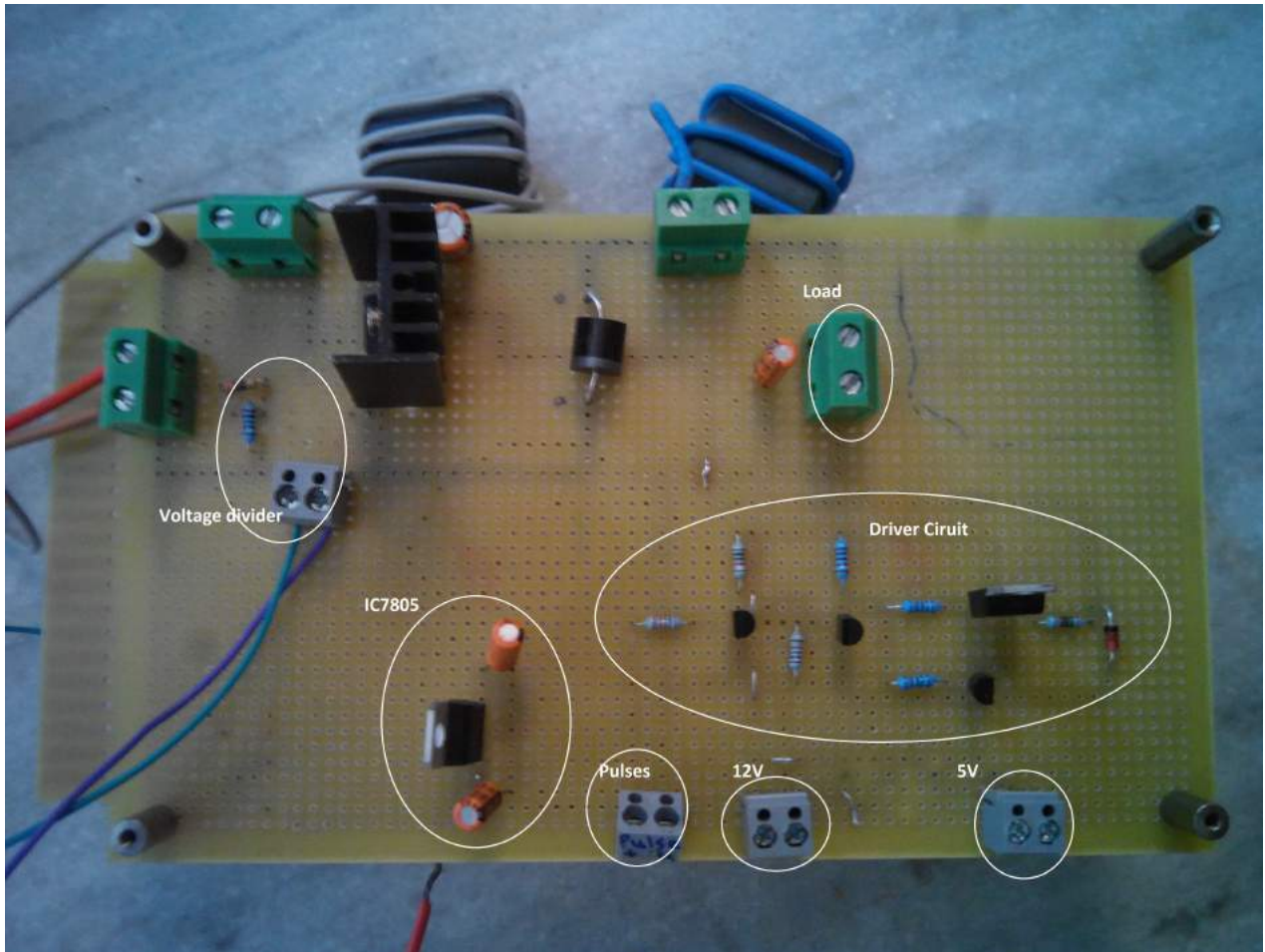
- [9] Dr. Mutlu Boztepe, DC-DC Converters EE328 Power Electronics, Department of Electrical and Electronics Engineering - Ege University.
- [10] Saravana Selvan. D, "Modeling and Simulation of Incremental Conductance MPPT Algorithm for Photovoltaic Applications", International Journal of Scientific Engineering and Technology (ISSN : 2277-1581) Volume No.2, Issue No.7, July 2013.
- [11] D. C. Riawan and C. V. Nayar, "Design and Implementation of P/I-Based MPPT for Wide Temperature Range Operation," presented at Renewable Energy For Sustainable Development, Perth, Western Australia, 2006

Appendix Hardware Setup

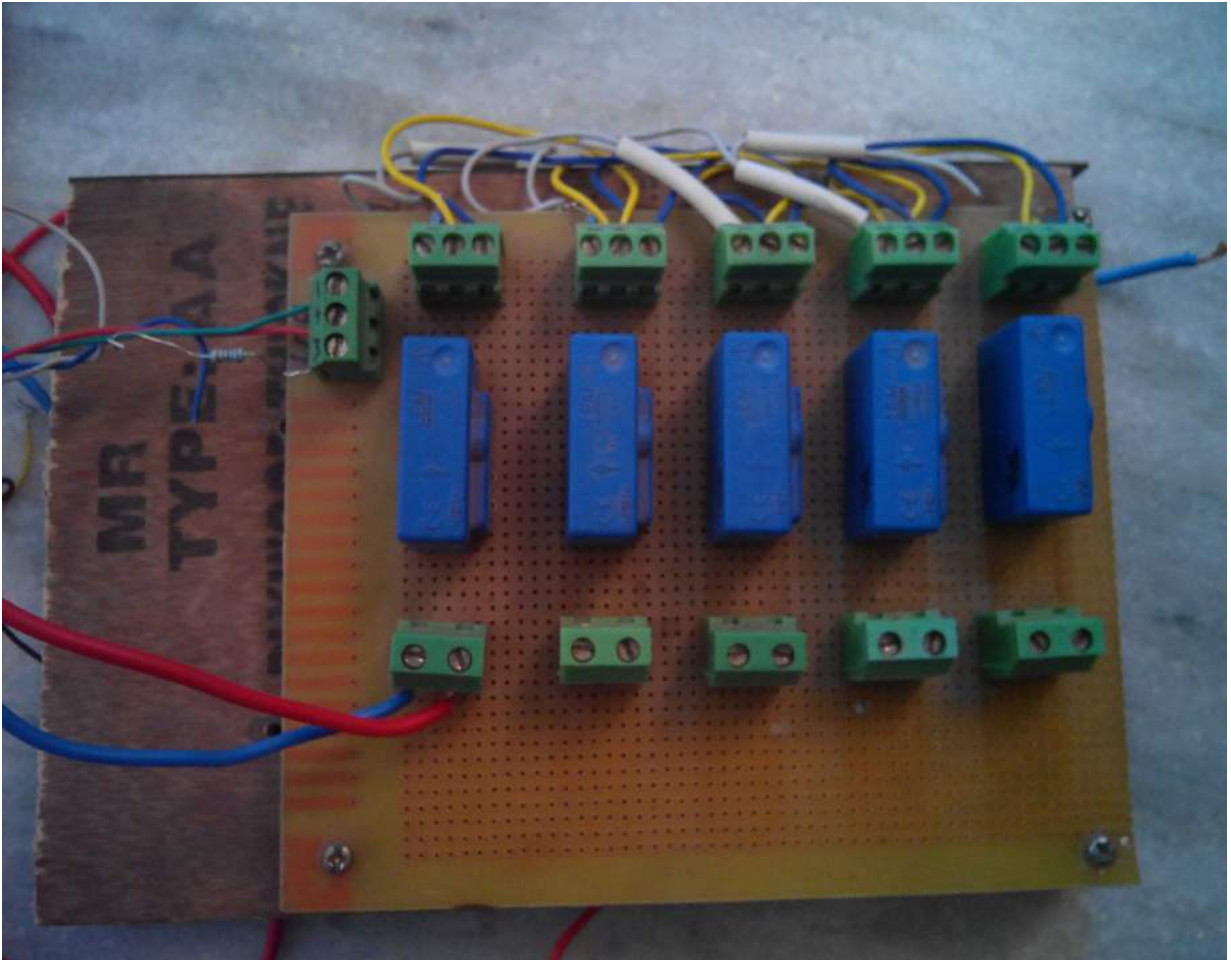


Hardware Implementation of PIC controller

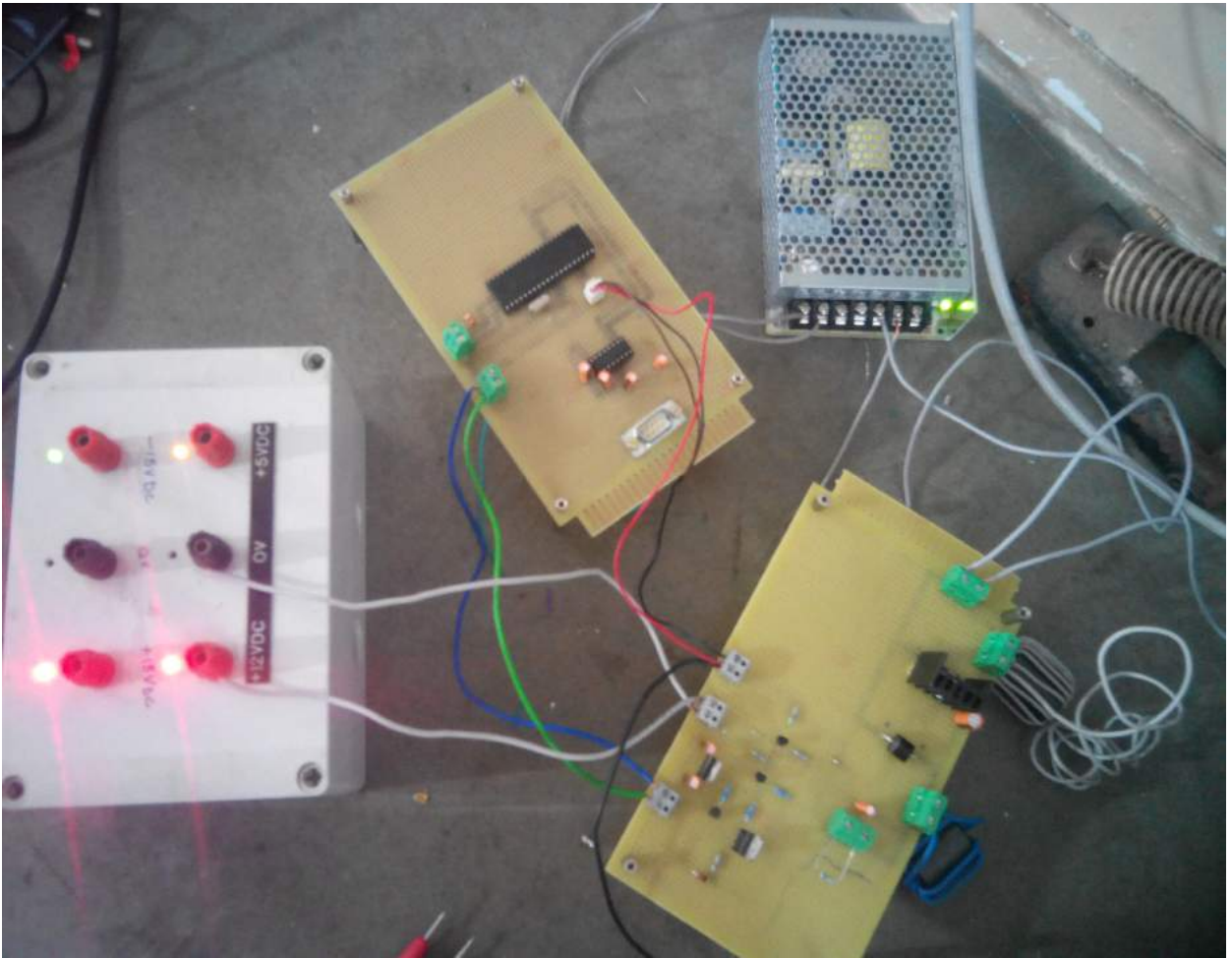
-



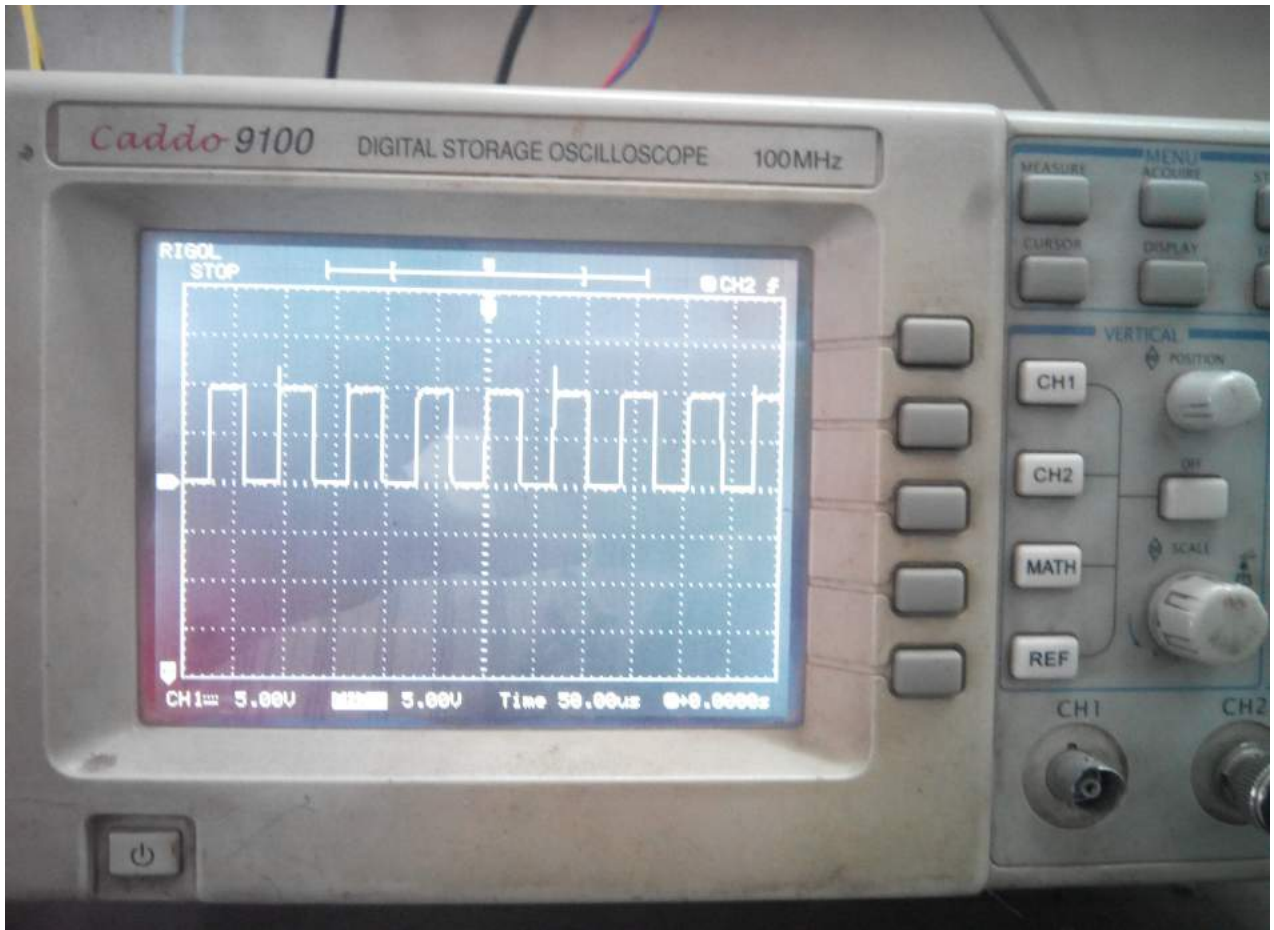
Hardware Implementation of Cuk Converter



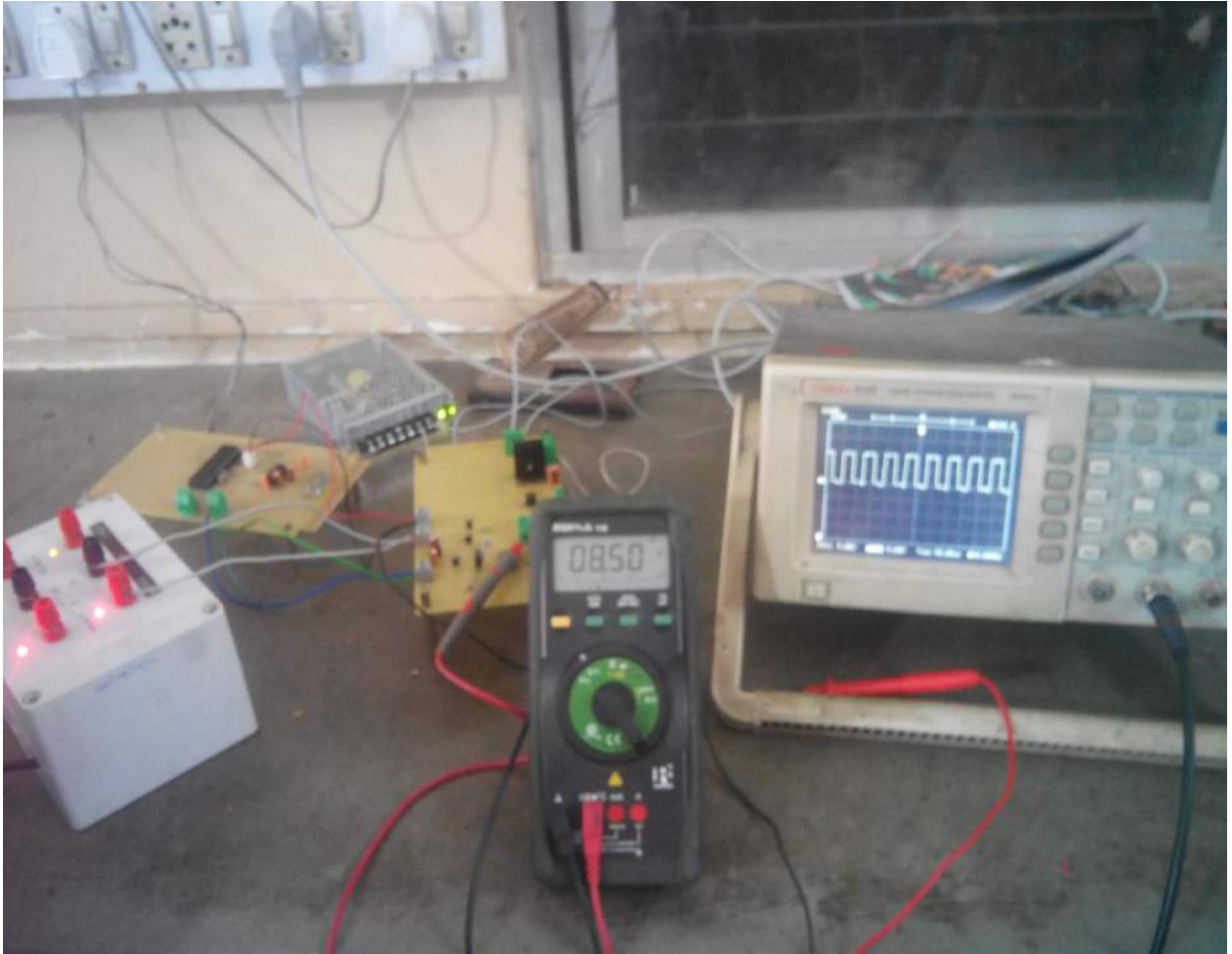
LEM current sensor LA 25-NP



Industry test set up



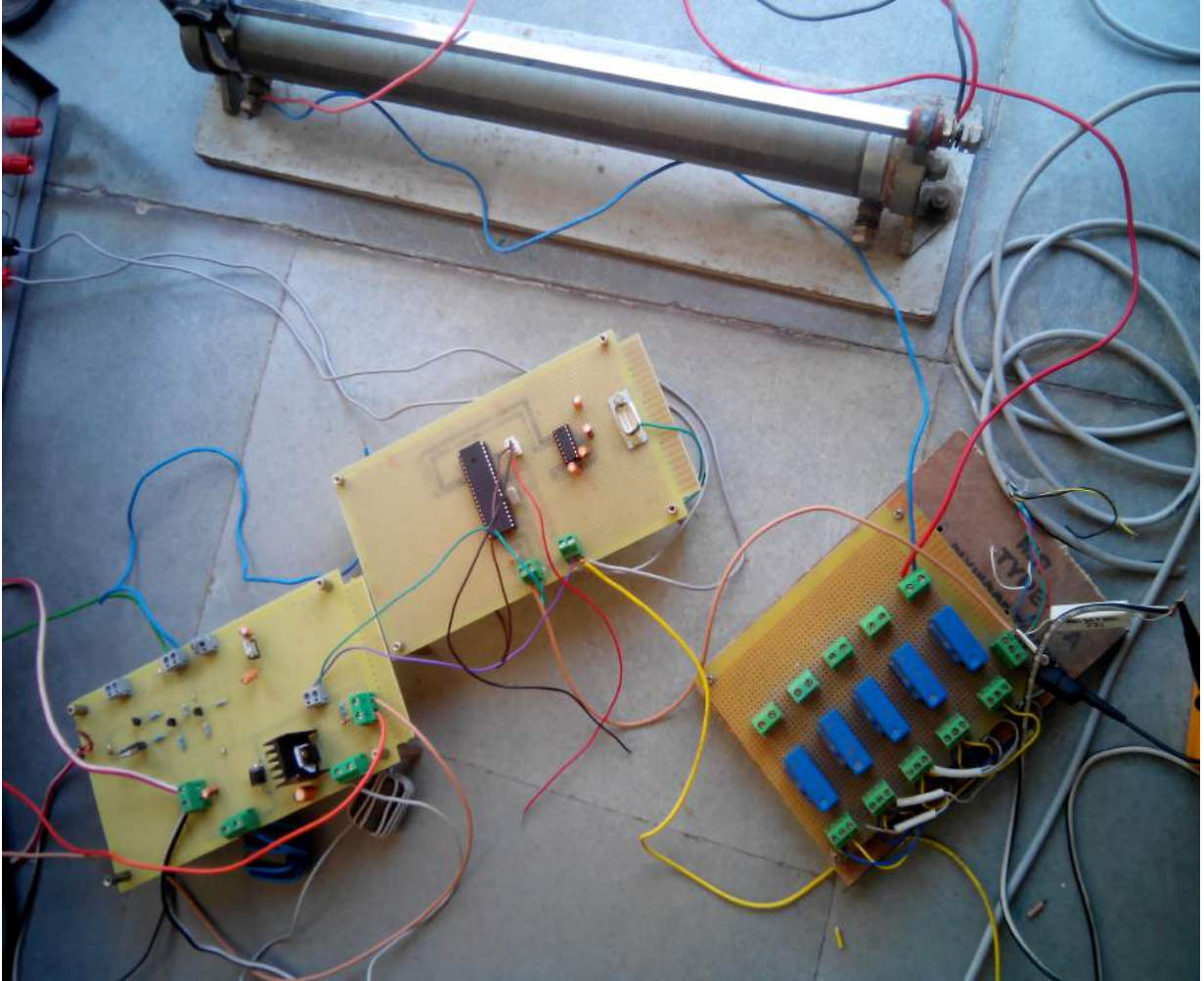
Duty cycle obtained from driver circuit



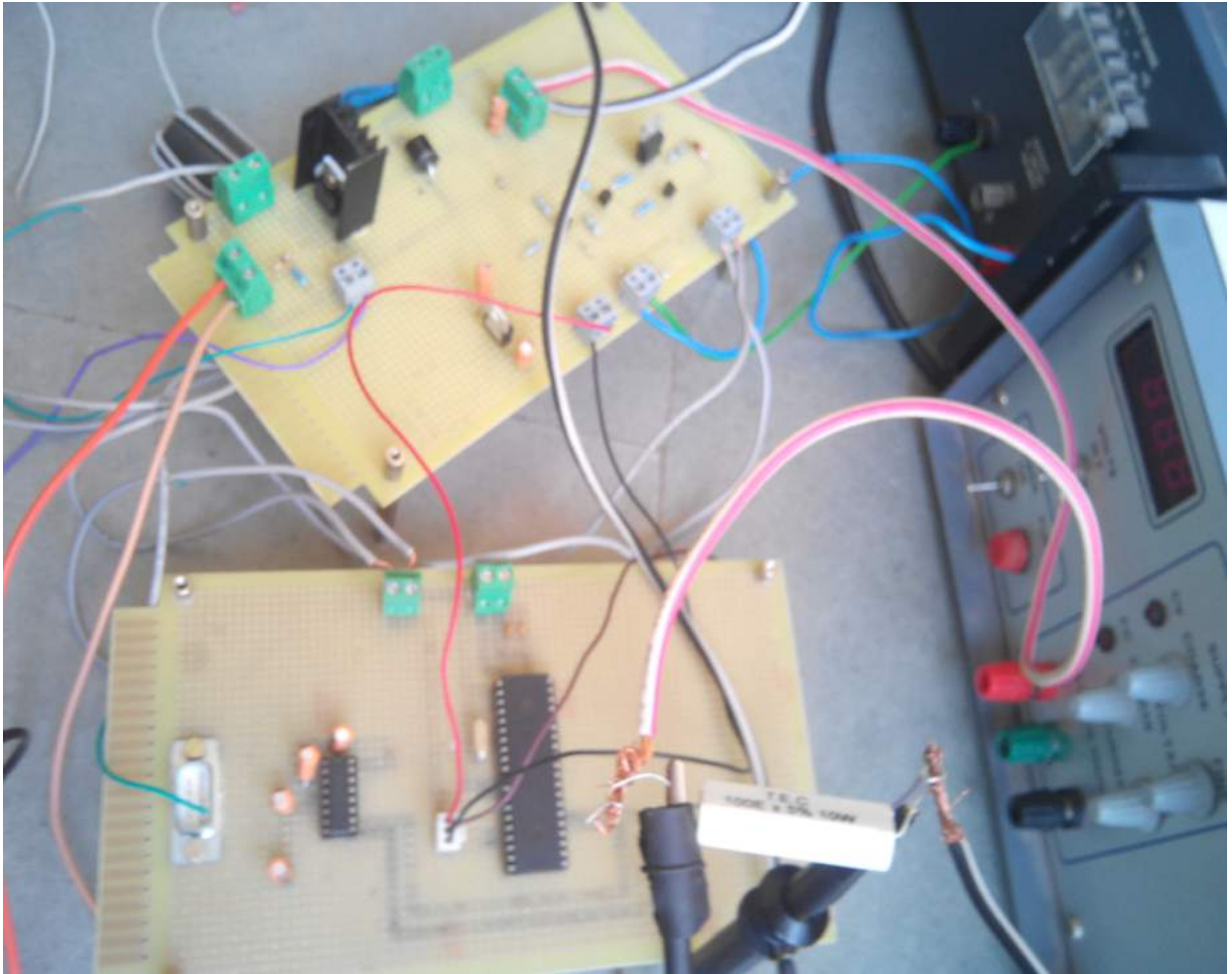
Tested output of the Cuk Converter



Hardware connected with Solar Panel



The whole set up connected along with current sensor



Load connected at the output of the Cuk Converter